Published Online: 26 July, 2018 | Supp Info: http://doi.org/10.1084/jem.20172359
Downloaded from jem.rupress.org on July 29, 2018

JEM Journal of Experimental Medicine

ARTICLE

ICAM-1 controls development and function of ILC2

Ai-Hua Lei[1,2]*, Qiang Xiao[1,2]*, Gao-Yu Liu[2], Kun Shi[3], Qiong Yang[2], Xing Li[4], Yu-Feng Liu[2], Hai-Kun Wang[5], Wei-Ping Cai[6], Yu-Juan Guan[6], Dmitry I. Gabrilovich[2,7,8], and Jie Zhou[1,2,8]

Group 2 innate lymphoid cells (ILC2s) are emerging as key players in the pathogenesis of allergic airway inflammation. The mechanisms regulating ILC2, however, are not fully understood. Here, we found that ICAM-1 is required for the development and function of ILC2. ICAM-1–deficient (*ICAM-1*$^{-/-}$) mice displayed significantly lower levels of ILC2s in the bone marrow and peripheral tissues than wild-type controls. CLP transfer and in vitro culture assays revealed that the regulation of ILC2 by ICAM-1 is cell intrinsic. Furthermore, ILC2s from *ICAM-1*$^{-/-}$ mice were functionally impaired, as indicated by the diminished production of type-2 cytokines in response to IL-33 challenge. The reduction in lung ILC2s caused a clear remission of airway inflammation in *ICAM-1*$^{-/-}$ mice after administration of papain or *Alternaria alternata*. We further demonstrate that ILC2 defects caused by ICAM-1 deficiency are due to ERK signaling-dependent down-regulation of GATA3 protein. Collectively, these observations identify ICAM-1 as a novel regulator of ILC2.

Introduction

Group 2 innate lymphoid cells (ILC2s) do not express antigen-specific receptors. However, similar to CD4 T cells, they produce type-2 cytokines, including IL-5 and IL-13, when exposed to epithelium-derived cytokines such as IL-33, IL-25, and thymic stromal lymphopoietin (Halim et al., 2012a; Walker et al., 2013; Martinez-Gonzalez et al., 2015; Klose and Artis, 2016). In adult mice, ILC2s develop from common lymphoid progenitors (CLPs) in the bone marrow (BM), followed by $\alpha_4\beta_7^+$ lymphoid progenitors (α-LP), common helper-like ILC progenitors (ChILP), and finally differentiate into ILC2 precursors (ILC2P; Serafini et al., 2015; Zook and Kee, 2016). ILC2s have been found in mucous tissues (lung and intestine), nonlymphoid organs (liver, kidney, and visceral adipose tissue), lymphoid tissues (spleen, BM, and mesenteric lymph node [mLN]), and blood (Walker et al., 2013; Brestoff et al., 2015; Serafini et al., 2015; Riedel et al., 2017; Karta et al., 2018). ILC2s have been shown to be important in inflammation, tissue remodeling, metabolism, and thermal homeostasis; however, their function depends on the tissue they reside and the pathological conditions (McKenzie et al., 2014; Artis and Spits, 2015; Lee et al., 2015). Notably, lung ILC2s play a crucial role in promoting allergic airway inflammation during innate immune responses (Halim et al., 2014; Martinez-Gonzalez et al., 2015).

In recent years, the transcriptional programs and signaling molecules that control the development, homeostasis, and function of ILC2s have been extensively studied (Ebbo et al., 2017; Zhong and Zhu, 2017). GATA3 is a key regulator of ILC2s (Hoyler et al., 2012; Mjösberg et al., 2012). Other transcription factors such as RORα (Halim et al., 2012b; Wong et al., 2012), TCF-1 (Yang et al., 2013), Gfi1 (Spooner et al., 2013), G9a (Antignano et al., 2016), and Ets1 (Zook et al., 2016) also contribute to the regulation of ILC2 development and/or function. Very recently, it was reported that ILC2s express certain costimulation molecules such as ICOS and PD-1, which regulate ILC2 function through STAT5 signaling (Maazi et al., 2015; Taylor et al., 2017). These results suggest a potential role of costimulation molecules in ILC2 function.

Intercellular cell adhesion molecule-1 (ICAM-1 or CD54), which primarily interacts with leukocyte function-associated molecule (LFA)–1, is a transmembrane glycoprotein receptor of the immunoglobulin superfamily (Stanciu and Djukanovic, 1998; Hogg et al., 2011). It is broadly expressed in many cell types, including T cells, B cells, neutrophils, endothelial cells, and epithelial cells (Stanciu and Djukanovic, 1998). Apart from its role in mediating the adhesion of inflammatory cells to the vascular endothelium, epithelium, and extracellular matrix, ICAM-1 also functions as a costimulation molecule to assist tight

[1]Joint Program in Immunology, Department of Internal Medicine, Affiliated Guangzhou Women and Children's Medical Center, Zhongshan School of Medicine, Sun Yat-sen University, Guangzhou, China; [2]Institute of Human Virology, Zhongshan School of Medicine, Sun Yat-sen University, Guangzhou, China; [3]Department of Gynecology, Guangzhou Women and Children's Medical Center, Guangzhou, China; [4]Department of Medical Oncology and Guangdong Key Laboratory of Liver Disease, the Third Affiliated Hospital of Sun Yat-sen University, Guangzhou, China; [5]CAS Key Laboratory of Molecular Virology and Immunology, Institut Pasteur of Shanghai, Chinese Academy of Sciences, Shanghai, China; [6]Guangzhou No.8 Hospital, Guangzhou, China; [7]The Wistar Institute, Philadelphia, PA; [8]Key Laboratory of Tropical Disease Control, Chinese Ministry of Education, Sun Yat-sen University, Guangzhou, China.

*A.-H. Lei and Q. Xiao contributed equally to this paper; Correspondence to Jie Zhou: zhouj72@mail.sysu.edu.cn.

© 2018 Lei et al. This article is distributed under the terms of an Attribution–Noncommercial–Share Alike–No Mirror Sites license for the first six months after the publication date (see http://www.rupress.org/terms/). After six months it is available under a Creative Commons License (Attribution–Noncommercial–Share Alike 4.0 International license, as described at https://creativecommons.org/licenses/by-nc-sa/4.0/).

cell-to-cell interactions and outside-in signal signaling transduction (Springer, 1990; Dustin et al., 2004). For instance, the costimulation of ICAM-1 by LFA-1 causes T cell activation during antigen presentation (Stanciu and Djukanovic, 1998). Interestingly, ICAM-1 has been shown to participate in the pathogenesis of asthma and may therefore be a potential target for asthma treatment (Stanciu and Djukanovic, 1998; Li et al., 2005; Furusho et al., 2006; Mukhopadhyay et al., 2014). Asthma patients showed an increased expression of ICAM-1 on T cells (De Rose et al., 1994; Stanciu and Djukanovic, 1998). The level of soluble ICAM-1 in the serum and bronchoalveolar lavage (BAL) fluid was elevated in asthma patients (Lee et al., 1997; Tang et al., 2002; Bijanzadeh et al., 2009). Furthermore, ICAM-1 deficiency has been shown to attenuate airway inflammation in mice (Hatfield et al., 1997; Wolyniec et al., 1998; Tang and Fiscus, 2001). Blocking the interaction between ICAM-1 and LFA-1 impaired Th2 responses and allergic airway inflammation (Wegner et al., 1990; Nakao et al., 1994; Iwamoto and Nakao, 1995). However, contrasting results have been reported by different groups (Nakajima et al., 1994; Salomon and Bluestone, 1998). A very recent study showed that β2 integrin (CD18), a subunit of LFA-1, is required for the trafficking of ILC2s into the lungs (Karta et al., 2018). However, the role of ICAM-1 in the biological function of ILC2s remains largely unknown.

In this study, we attempted to explore the relationship between ICAM-1 and the development and function of ILC2s. ILC2s and their progenitors expressed high levels of ICAM-1 and its ligand LFA-1. IL-33 stimulation enhanced ICAM-1 expression on both mouse and human ILC2s. ICAM-1 deficiency impaired ILC2 development and function, which contributed to the attenuation of allergic inflammation in the lungs. Further studies revealed that dysregulation of the GATA3 protein, via ERK signaling pathway, represented the underlying mechanism.

Results

ICAM-1 is required for the development of ILC2s

To investigate the role of ICAM-1 in the development of ILC2s, we first analyzed its expression on ILC2s ($CD45^+Lin^-CD90.2^+CD25^+GATA3^{high}ST2^+$) and their distinct progenitors, including CLPs ($CD45^+Lin^-CD127^+\alpha4\beta7^-Flt3^+$), α-LPs ($CD45^+Lin^-CD127^+\alpha4\beta7^+Flt3^-$), ChILPs ($CD45^+Lin^-CD127^+\alpha4\beta7^+Flt3^-CD25^-$), and ILC2Ps ($CD45^+Lin^-CD127^+\alpha4\beta7^+Flt3^-CD25^+$) as described (Yu et al., 2014; Maazi et al., 2015; Antignano et al., 2016; Monticelli et al., 2016). The gating strategies of flow cytometry are shown in Fig. S1, A and B. $CD4^+$ T cells were analyzed in parallel. Results showed that mature ILC2s and their progenitors expressed higher levels of ICAM-1 than $CD4^+$ T cells (Fig. 1, A and B). Furthermore, α-LPs and ILC2Ps displayed higher levels of ICAM-1 than CLPs and ChILPs (Fig. 1, A and B). Interestingly, LFA-1, the ligand of ICAM-1, showed a similar expression pattern (Fig. S1 C). This dynamic expression pattern of ICAM-1 indicates its potential role in the development of ILC2.

We next examined the levels of immature ILC2s (iILC2) in the BM of WT and ICAM-1–deficient (*ICAM-1*$^{-/-}$) mice by flow cytometric analysis of $CD45^+Lin^-Sca\text{-}1^{high}c\text{-}kit^{low}CD127^+CD25^+$ cells (Halim et al., 2012a; Hoyler et al., 2012; Antignano et al., 2016). It was found that both the frequency and absolute number of iILC2s in *ICAM-1*$^{-/-}$ mice were reduced to ∼30% of those in the WT littermates (Fig. 1, C and D). Alternatively, BM iILC2s defined as $CD45^+Lin^-CD127^+Flt3^-\alpha4\beta7^+CD90.2^+$ produced a similar result (Fig. S1 D). ILC2s could be expanded in vivo through the administration of IL-33 (Spooner et al., 2013; Antignano et al., 2016). As expected, intraperitoneal injection of IL-33 caused a pronounced increase in the number of BM iILC2s in both WT and *ICAM-1*$^{-/-}$ mice, whereas their levels were persistently lower in *ICAM-1*$^{-/-}$ than WT controls (Fig. 1 E). Further analysis revealed that the frequencies of α-LPs, ChILPs, and ILC2Ps were significantly lower in *ICAM-1*$^{-/-}$ BM than in WT controls (Fig. 1 F). These observations indicated that ICAM-1 is required for the development of ILC2s.

To investigate whether the lower levels of ILC2s in *ICAM-1*$^{-/-}$ mice were caused by developmental defects, CLPs from *ICAM-1*$^{-/-}$ ($CD45.2^+$) and WT ($CD45.1/2^+$) mice were mixed at 1:1 ratio and transferred into immunodeficient nonobese diabetic (NOD)–$Prkdc^{em26Cd52}Il2rg^{em26Cd22}$/Nju (NCG) ($CD45.1^+$)-mice (Cao et al., 2017), which lack T cells, B cells, and ILC2s, as confirmed by flow cytometry (Fig. S1 E). 3 wk later, flow cytometric analysis revealed that the majority of ILC2s in the recipients, both in the BM (77% ± 0.1280 in WT vs. 23% ± 0.1280 in *ICAM-1*$^{-/-}$) and the lungs (74.9% ± 0.1513 in WT vs. 20.5% ± 0.1234 in *ICAM-1*$^{-/-}$), were derived from WT CLPs (Fig. 1, G and H). Even though the development of B cells and NK cells from CLPs was not affected by ICAM-1 deletion, the generation of thymic T cells was clearly impaired by the absence of ICAM-1 (Fig. 1 H), which was consistent with previous reports (Fine and Kruisbeek, 1991; Scholer et al., 2008). The capability of CLP homing to BM was comparable between *ICAM-1*$^{-/-}$ and WT controls (Fig. S1 F). These results indicated that the loss of ICAM-1 impaired the differentiation of CLPs into ILC2s. For further confirmation, we performed in vitro differentiation of CLPs into ILC2s, as described previously (Seehus et al., 2015; Seehus and Kaye, 2016; Koga et al., 2018). After a 9–10-d co-culture with OP9-DL1 cell line, WT CLPs efficiently differentiated into ILC2s ($CD45^+Lin^-ICOS^+CD25^+$) as expected; however, the differentiation of *ICAM-1*$^{-/-}$ CLPs into ILC2 was dramatically diminished in the presence or absence of IL-33 (Fig. 1 I and Fig. S1 G). As expected, the development of B cells from *ICAM-1*$^{-/-}$ CLPs did not display any defect after co-culture with the OP9 cell line (Fig. S1 H). Importantly, administration of blocking antibodies against ICAM-1 or its ligand CD11a (a subunit of LFA-1) significantly diminished the generation of ILC2 from WT CLP in vitro with or without IL-33 (Fig. 1 J and Fig. S1 I), whereas B cell differentiation was not affected (Fig. S1 I). Moreover, the OP9-DL1 cell line or BM stroma cells did not express LFA-1, whereas CLPs expressed a relatively higher level of LFA-1 (Fig. S1 J). Furthermore, neither apoptosis (Fig. S1 K) nor proliferation (Fig. S1 L) of BM iILC2s was affected by ICAM-1 deletion. These observations indicated that ICAM-1 regulates the development of ILC2s in a cell-intrinsic manner.

Loss of ICAM-1 reduces tissue ILC2s

Given that ICAM-1 deficiency impairs the development of iILC2s, we speculated that there would be lower levels of ILC2s in the peripheral tissues of *ICAM-1*$^{-/-}$ mice. We defined tissue-resident

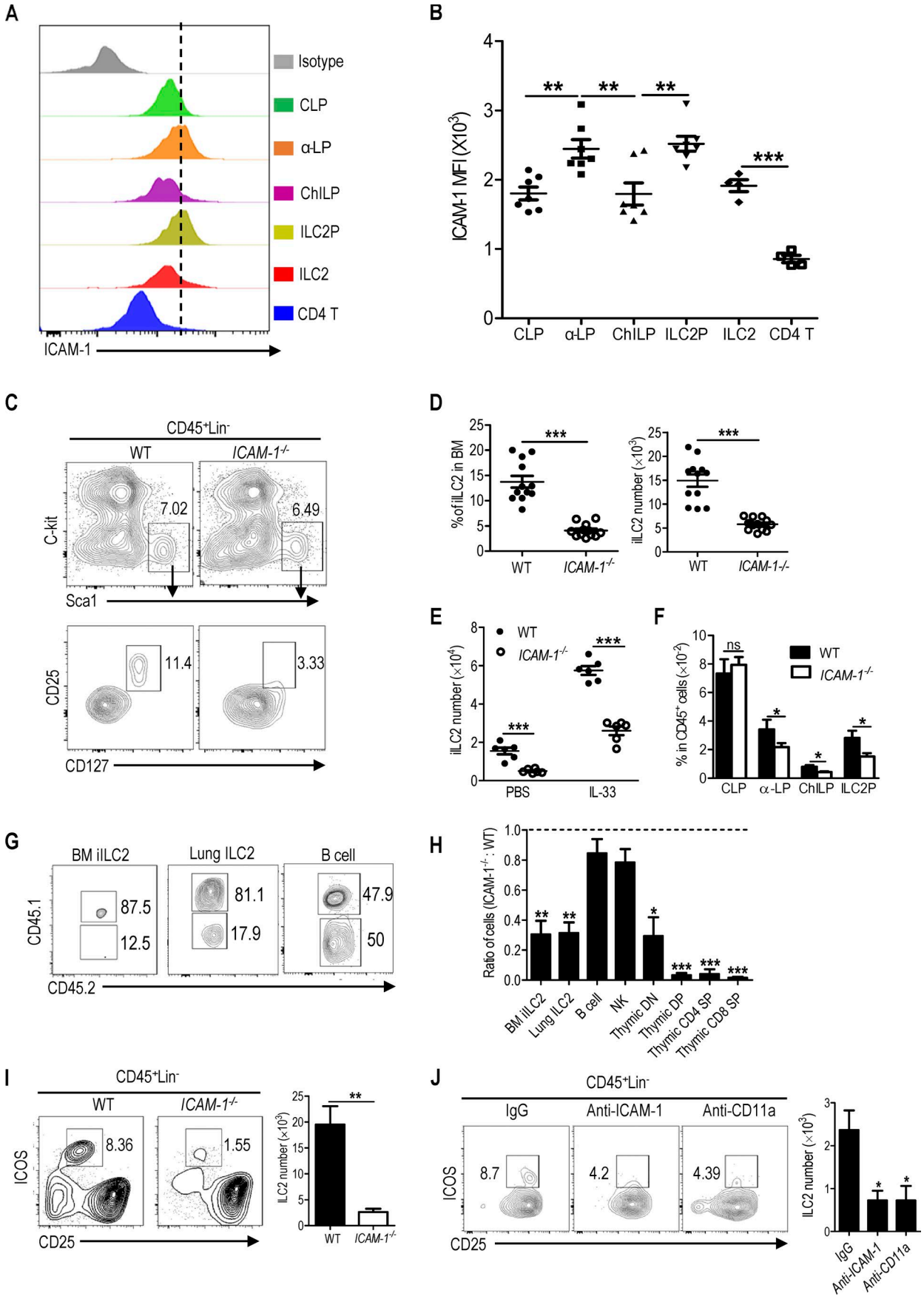
A
Isotype
CLP
α-LP
ChILP
ILC2P
ILC2
CD4 T
ICAM-1
B
ICAM-1 MFI (X10³)
CLP
α-LP
ChILP
ILC2P
ILC2
CD4 T
C
CD45⁺Lin⁻
WT
ICAM-1⁻/⁻
C-kit
Sca1
7.02
6.49
CD25
CD127
11.4
3.33
D
% of iILC2 in BM
iILC2 number (×10³)
WT
ICAM-1⁻/⁻
E
iILC2 number (×10⁴)
PBS
IL-33
F
% in CD45⁺ cells (×10⁻²)
ns
CLP
α-LP
ChILP
ILC2P
G
BM iILC2
Lung ILC2
B cell
CD45.1
CD45.2
87.5
12.5
81.1
17.9
47.9
50
H
Ratio of cells (ICAM-1⁻/⁻ : WT)
BM iILC2
Lung ILC2
B cell
NK
Thymic DN
Thymic DP
Thymic CD4 SP
Thymic CD8 SP
I
CD45⁺Lin⁻
WT
ICAM-1⁻/⁻
ICOS
CD25
8.36
1.55
ILC2 number (×10³)
J
CD45⁺Lin⁻
IgG
Anti-ICAM-1
Anti-CD11a
ICOS
CD25
8.7
4.2
4.39
ILC2 number (×10³)

ILC2 as CD45$^+$Lin$^-$CD90.2$^+$CD127$^+$GATA3$^+$ cells in the mLN, small intestine, and large intestine as described previously (Geiger et al., 2014). Lung ILC2 was gated as CD45$^+$Lin$^-$CD90.2$^+$CD25$^+$, which were GATA3^{high}ST2$^+$ cells as presented in Fig. S1 A. Results showed that both the frequencies and absolute cell numbers of ILC2s were dramatically decreased in multiple tissues of *ICAM-1*$^{-/-}$ mice, when compared with those in WT littermates (Fig. 2, A and B). All tissue ILC2s expressed CD69 (Fig. 2 C; Roediger et al., 2013). The reduction of lung ILC2 was further confirmed (Fig. S2 A), by using alternative gating strategy (CD45$^+$Lin$^-$CD90.2$^+$ST2$^+$) as previously described (Seehus et al., 2015). It is worth noting that although high levels of ICAM-1 expression were observed in NK, ILC1, and ILC3 subsets (Fig. 2 D), their frequencies were not significantly different between *ICAM-1*$^{-/-}$ and WT mice (Fig. 2, E–G). These observations indicated that ICAM-1 deficiency specifically impaired the level of tissue ILC2s.

ICAM-1 is required for the function of ILC2s

IL-33 is the key cytokine that drives the functional activation of ILC2s (Hoyler et al., 2012; Zook et al., 2016). We first investigated the potential link between IL-33 signaling and ICAM-1 expression. Interestingly, IL-33 stimulation caused a clear induction of ICAM-1 expression on mouse iILC2s (Fig. 3 A), whereas no effect was observed on its ligand LFA-1 (Fig. 3 B). Similar results were obtained for human ILC2s (Fig. 3 C), which were defined as CD45$^+$Lin$^-$CD127$^+$CRTH2$^+$ cells (Fig. S2 B; Chang et al., 2014) and expressed ICAM-1 and LFA-1 (Fig. S2 C). To investigate the effect of ICAM-1 on ILC2 function, equal number of lung ILC2s from WT and *ICAM-1*$^{-/-}$ mice were sorted and cultured for 3 d in the presence of IL-2, IL-7, and IL-33. The amount of IL-5 and IL-13 in the supernatants of *ICAM-1*$^{-/-}$ ILC2s were approximately sixfold lower than that in the supernatants of WT controls (Fig. 3 D). Purified BM iILC2 culture of in the presence of IL-2, IL-7, and IL-33 presented the similar results, including lower proportion of IL-5$^+$ IL-13$^+$ ILC2 (Fig. S2 D), as well as lower amount of IL-5 and IL-13 in the supernatant (Fig. S2 E), from *ICAM-1*$^{-/-}$ ILC2s. These results suggested that loss of ICAM-1 impaired the function of ILC2s.

Subsequently, we performed an in vivo IL-33 challenge. As expected, intranasal administration of IL-33 significantly increased the number of lung ILC2s in both WT and *ICAM-1*$^{-/-}$ mice (Fig. 3 E); their levels in *ICAM-1*$^{-/-}$ mice were consistently lower than WT mice upon IL-33 treatment (Fig. 3 E). Particularly, the production of IL-5 and IL-13 by *ICAM-1*$^{-/-}$ ILC2s was less than half of that by WT ILC2s after IL-33 challenge (Fig. 3 F). As further support, the amounts of IL-5 and IL-13 (Fig. 3 G), airway eosinophilic infiltration (Fig. 3 H), in the BAL fluid were apparently reduced in *ICAM-1*$^{-/-}$ mice. The attenuation of lung inflammation was further confirmed by H&E staining (Fig. 3 I). These results suggested that the function of *ICAM-1*$^{-/-}$ ILC2s was compromised in response to IL-33 stimulation.

For further confirmation, equal number of lung ILC2s from WT and *ICAM-1*$^{-/-}$ mice were adoptively transferred to immunodeficient NCG mice, followed by intranasal administration of IL-33 for 3 d (Fig. 4 A). Results revealed a comparable number of ILC2s in the lungs of recipients receiving WT and *ICAM-1*$^{-/-}$ ILC2s (Fig. 4 B), suggesting that the migration or survival of ILC2s may be not apparently affected by ICAM-1 deletion.

Notably, the total CD45$^+$ immune cells in the BAL fluid (Fig. 4 C), the infiltrated eosinophils (Fig. 4 D) and the amount of IL-5 and IL-13 (Fig. 4 E) in the BAL, were significantly lower in the recipients of *ICAM-1*$^{-/-}$ ILC2s than the controls receiving WT ILC2s. The attenuation of lung inflammation in the recipients of *ICAM-1*$^{-/-}$ ILC2s was verified by H&E staining (Fig. 4 F). The protease papain has been widely used to induce type 2 airway inflammation, in which ILC2 is the major driver (Yang et al., 2013; Antignano et al., 2016; Monticelli et al., 2016). A 3-d intranasal instillation of papain was further performed in NCG mice after transfer with WT or *ICAM-1*$^{-/-}$ ILC2. Similar results were observed (Fig. 4, G–J), although the airway inflammation was less affected, when compared with IL-33 challenge. Collectively, these observations demonstrated that ICAM-1 is required for the function of ILC2s.

We further evaluated the function of other ILC subsets by using a dextran sulfate sodium (DSS)–induced murine colitis model (Mielke et al., 2013; Wang et al., 2017). Consistent with a previous report (Bendjelloul et al., 2000), ICAM-1 deficiency attenuated DSS-induced colitis, indicated by milder body weight loss and less shortened colon length (Fig. S2, F and G). Flow cytometric analysis showed that the production of IFN-γ by ILC1 in colon (Fig. S2 H), that of IL-22, IL-17A, and IFN-γ by ILC3 in colon (Fig. S2 I), displayed no differences between WT and *ICAM-1*$^{-/-}$ mice. These observations indicate that ICAM-1 deficiency did not affect the function of other ILC subsets.

Figure 1. **ICAM-1 controls the development of ILC2. (A)** Representative flow cytometric analysis of ICAM-1 expression on distinct ILC progenitor subsets in the BM and ILC2, as well as CD4$^+$ T cells in lung from mice. **(B)** The mean fluorescence intensity (MFI) levels of ICAM-1 from A were shown (n = 4–7). **(C)** Representative flow cytometric analysis of iILC2, pregated on CD45$^+$Lin$^-$ in BM from WT and *ICAM-1*$^{-/-}$ mice. **(D)** The frequencies and number of iILC2 from C (n = 12). **(E)** Quantification of iILC2 in BM from WT and *ICAM-1*$^{-/-}$ mice after intraperitoneal injection with IL-33 or vehicle PBS (n = 6 per group). **(F)** The frequencies of CLP, α-LP, ChILP, and ILC2P among CD45$^+$ cells in BM from WT and *ICAM-1*$^{-/-}$ mice (n = 6 per phenotype). **(G and H)** CLPs from WT (CD45.1/2$^+$) and *ICAM-1*$^{-/-}$ (CD45.2$^+$) mice were mixed at 1:1 ratio, followed by intravenously transferred into NCG (CD45.1$^+$) mice (n = 6). 3 wk after transplantation, the levels of BM iILC2 (CD45$^+$Lin$^-$C-kit^{low}Sca1^{high}CD127$^+$CD25$^+$), lung ILC2 (CD45$^+$Lin$^-$CD90.2$^+$CD25$^+$) and BM B cells (CD19$^+$B220$^+$) from WT (CD45.1/2$^+$) and *ICAM-1*$^{-/-}$ (CD45.1$^-$CD45.2$^+$) was evaluated by flow cytometry (G). The ratio of *ICAM-1*$^{-/-}$ to WT donor cells (*ICAM-1*$^{-/-}$/WT) among the indicated cell types, including BM iILC2, lung ILC2, B cells, spleen NK (CD45$^+$Lin$^-$NKP46$^+$NK1.1$^+$) cells, thymic CD4$^-$CD8$^-$ (double negative, DN) cells, CD4$^+$CD8$^+$ (double positive, DP) cells, CD4$^+$CD8$^-$ (single positive, CD4 SP), and CD4$^-$CD8$^+$ (single positive, CD8 SP) cells were shown (H). Dashed line indicated the expected result in the absence of genotype bias. **(I)** CLPs from *ICAM-1*$^{-/-}$ or WT mice were co-cultured with OP9-DL1 cell line in the presence of IL-7 (20 ng/ml) and IL-33 (20 ng/ml) for 10 d, and the frequency of ILC2 (Lin$^-$CD45$^+$ICOS$^+$CD25^{low}) was evaluated by flow cytometry and the number of ILC2 after co-culture was shown. **(J)** WT CLP cells were co-cultured with OP9-DL1 as in (I), in the presence of indicated blocking antibodies (5 µg/ml). The representative frequencies of ILC2s, pregated on CD45$^+$Lin$^-$ cells and the number of ILC2 were shown. Data are representative of two (A, B, and E–H), three (I and J), or four (C and D) independent experiments. Error bars show mean ± SEM; *, P < 0.05; **, P < 0.01; ***, P < 0.001 by unpaired Student's t test. ns, not significant. Numbers within flow plots indicate percentage of cells gated, and arrows from outlined areas at top indicate gated cells analyzed below.

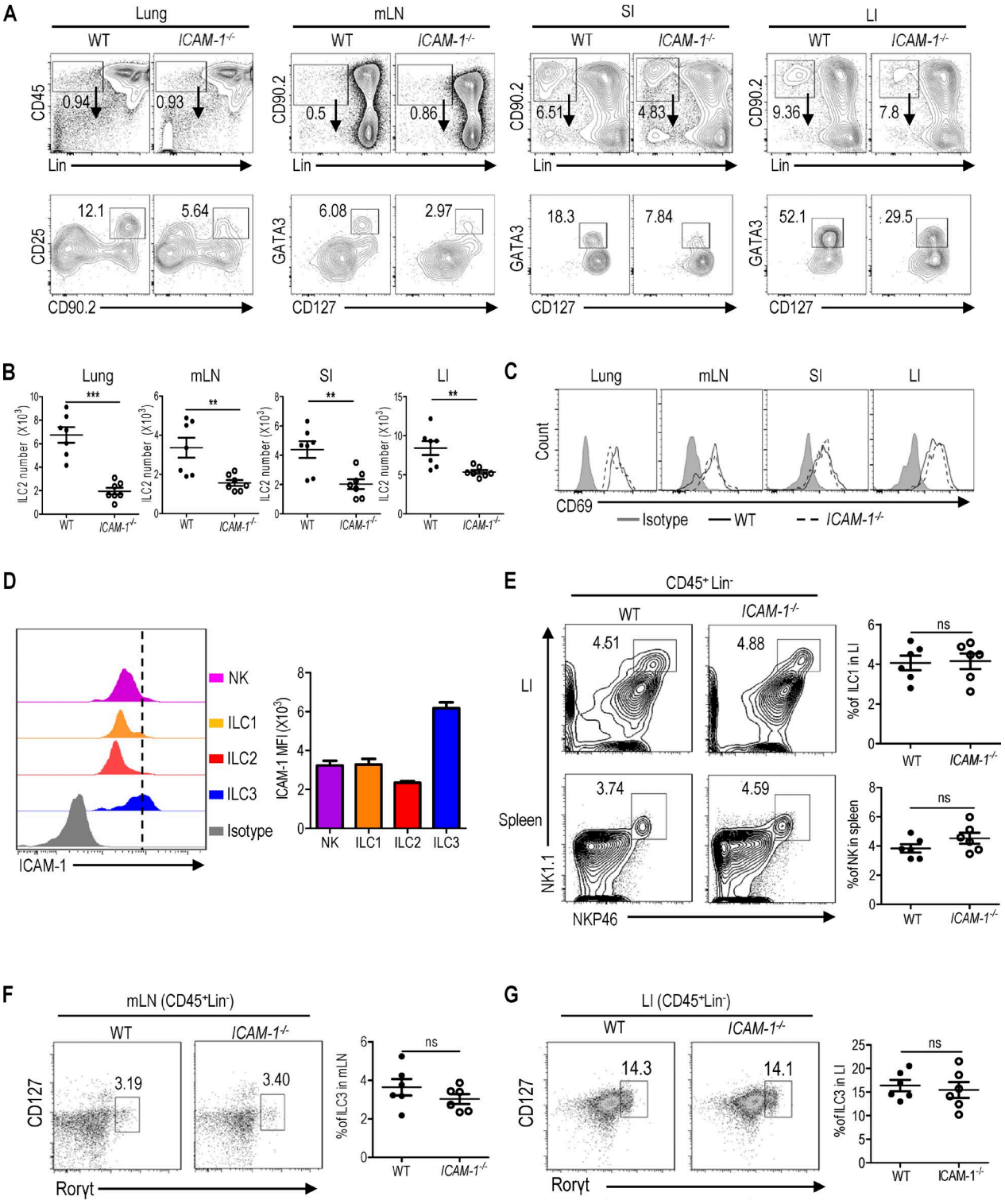

Figure 2. **Loss of ICAM-1 reduces tissue ILC2s. (A)** Representative flow cytometry plots of ILC2s in the peripheral tissues from WT and *ICAM-1*$^{-/-}$ mice, including lung (CD45$^+$Lin$^-$CD90.2$^+$CD25$^+$), mLN, lamina propria from small intestine (SI), and large intestine (LI; Lin$^-$CD90.2$^+$CD127$^+$GATA3$^+$, pregated on CD45$^+$ cells). **(B)** The number of ILC2s in A were shown (n = 7 per group). **(C)** Representative flow cytometric analysis of CD69 expression on tissue ILC2s from A. **(D)** Flow analysis of ICAM-1 expression on the indicated mouse ILC subsets, including spleen NK (CD45$^+$Lin$^-$NK1.1$^+$NKP46$^+$), ILC1 (CD45$^+$Lin$^-$NK1.1$^+$NKP46$^+$), ILC2 (CD45$^+$Lin$^-$CD127$^+$KLRG1$^+$), and ILC3 (CD45$^+$Lin$^-$CD127$^+$Roryt$^+$) in mLN. Mean fluorescence intensity (MFI) levels were shown (n = 6). **(E)** Frequencies of CD45$^+$Lin$^-$NK1.1$^+$NKP46$^+$ NK cells from spleen and CD45$^+$Lin$^-$NK1.1$^+$NKP46$^+$ ILC1s from LI in WT and *ICAM-1*$^{-/-}$ mice were determined by flow cytometry (n = 6 per group). **(F and G)** Frequencies of CD45$^+$Lin$^-$ CD127$^+$Roryt$^+$ ILC3s from mLN (F) and LI (G) of WT and *ICAM-1*$^{-/-}$ mice were determined by flow cytometry (n = 6 per group). Data are representative of two independent experiments. Error bars show mean ± SEM; **, P < 0.01; ***, P < 0.001 by unpaired Student's *t* test. ns, not significant. Numbers within flow plots indicate the percentages of cells gated, and arrows from outlined areas at top indicate gated cells analyzed below.

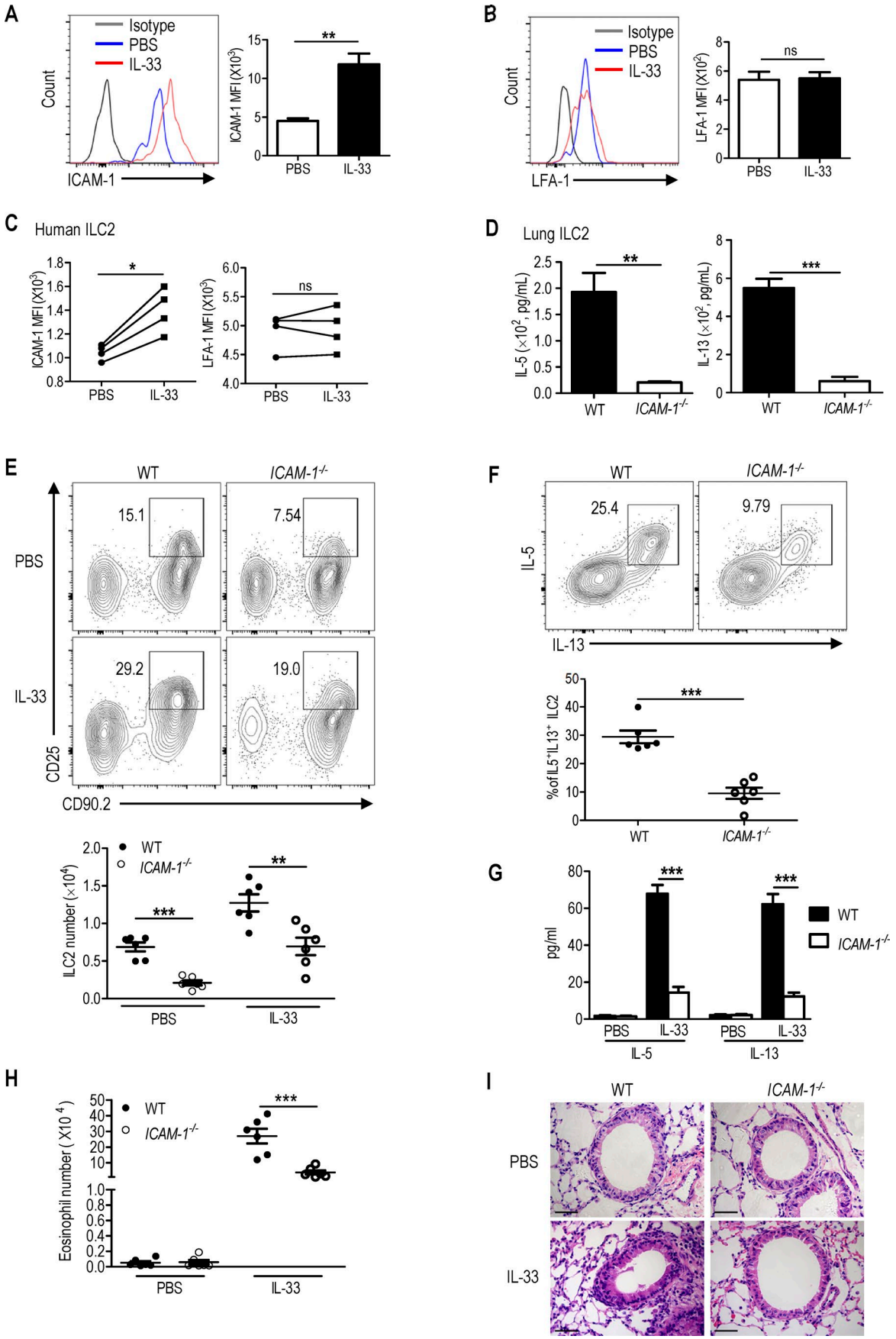
A
Isotype
PBS
IL-33
Count
ICAM-1
ICAM-1 MFI (X10³)
**
PBS
IL-33
B
Isotype
PBS
IL-33
Count
LFA-1
LFA-1 MFI (X10²)
ns
PBS
IL-33
C
Human ILC2
ICAM-1 MFI (X10³)
*
PBS
IL-33
LFA-1 MFI (X10³)
ns
PBS
IL-33
D
Lung ILC2
IL-5 (×10², pg/mL)
**
WT
ICAM-1-/-
IL-13 (×10², pg/mL)
***
WT
ICAM-1-/-
E
WT
ICAM-1-/-
PBS
IL-33
15.1
7.54
29.2
19.0
CD25
CD90.2
WT
ICAM-1-/-
ILC2 number (×10⁴)
***
**
PBS
IL-33
F
WT
ICAM-1-/-
IL-5
IL-13
25.4
9.79
%of IL5⁺IL13⁺ ILC2
***
WT
ICAM-1-/-
G
pg/ml
***
***
WT
ICAM-1-/-
PBS
IL-33
PBS
IL-33
IL-5
IL-13
H
WT
ICAM-1-/-
Eosinophil number (X10 ⁴)
***
PBS
IL-33
I
WT
ICAM-1-/-
PBS
IL-33

Loss of ICAM-1 attenuates ILC2-induced lung inflammation

Considering the importance of ILC2s in the induction of allergic airway inflammation (Ebbo et al., 2017), we further investigated whether loss of ICAM-1 affected ILC2-induced lung inflammation by 5-d intranasal instillation of papain. *ICAM-1*$^{-/-}$ mice showed significantly reduced influx of eosinophils (Fig. 5 A) and less production of type-2 cytokines (IL-5 and IL-13; Fig. 5 B) in BAL fluid than WT controls, after papain challenge. The remission of inflammation in *ICAM-1*$^{-/-}$ mice was further confirmed by H&E staining of lung tissues (Fig. 5 C). The frequency and number of ILC2s in the lungs (Fig. 5 D), as well as their capability to produce effector cytokines (Fig. 5 E), were consistently and significantly lower in *ICAM-1*$^{-/-}$ mice than those in WT controls. For further confirmation, *Alternaria alternata*, a clinically relevant allergen, was used to induce lung inflammation (Maazi et al., 2015). In line with the observations from papain model, the number of eosinophils (Fig. 5 F), the amount of IL-5 and IL-13 in the BAL (Fig. 5 G), the number of lung ILC2s (Fig. 5 H), and their production of effector cytokines (Fig. 5 I) were dramatically decreased in *ICAM-1*$^{-/-}$ mice. The attenuation of lung inflammation was confirmed by H&E staining (Fig. 5 J). These results demonstrated that ICAM-1 is critical for ILC2-mediated lung inflammation.

As both ILC2s and Th2 cells are known to contribute to lung inflammation (Halim et al., 2014; Walker and McKenzie, 2018), we further used OVA to induce lung inflammation in *ICAM-1*$^{-/-}$ and WT mice. Consistent with previous reports (Wolyniec et al., 1998; Tang and Fiscus, 2001), *ICAM-1*$^{-/-}$ mice showed diminished lung inflammation, as indicated by reduced eosinophils in the BAL (Fig. S3 A) and lung histology (Fig. S3 B). Moreover, Th2 cytokine-producing CD4$^+$ T cells were decreased in the lungs of *ICAM-1*$^{-/-}$ mice (Fig. S3 C). Of note, the number of lung ILC2s (Fig. S3 D) and their production of cytokines (Fig. S3 E) were also significantly reduced in *ICAM-1*$^{-/-}$ mice. It is therefore possible that reduction in both ILC2 and Th2 cell responses contribute to the remission of lung inflammation observed in *ICAM-1*$^{-/-}$ mice. Cross regulation between ILC2s and Th2 cells has also been reported (Mirchandani et al., 2014; Liu et al., 2015; Li et al., 2016). To eliminate the possible effect of CD4$^+$ T cells on ICAM-1-mediated ILC2 response, *ICAM-1*$^{-/-}$ mice were crossbred with *Rag-1*$^{-/-}$ mice to generate *ICAM-1*$^{-/-}$ *Rag-1*$^{-/-}$ mice. After papain treatment, the *ICAM-1*$^{-/-}$ *Rag-1*$^{-/-}$ mice showed consistently lower levels of eosinophils and type-2 cytokines in the BAL than the *Rag-1*$^{-/-}$ control mice (Fig. S3, F and G). As expected, the number of ILC2s and the frequency of IL-5$^+$IL-13$^+$ ILC2s in the lung were markedly reduced in *ICAM-1*$^{-/-}$ *Rag-1*$^{-/-}$ mice (Fig. S3, H and I). Lung inflammation was consequently, attenuated in *ICAM-1*$^{-/-}$ *Rag-1*$^{-/-}$ mice (Fig. S3 J). We therefore concluded that the regulation of ILC2s by ICAM-1 is independent of CD4 T cells.

Blocking the interaction between ICAM-1 and LFA-1 attenuates ILC2-mediated lung inflammation

As ICAM-1 primarily binds with LFA-1 (CD11a/CD18), we next investigated the effect of blocking the interaction between ICAM-1 and LFA-1 on ILC2-mediated lung inflammation. To this end, *Rag1*$^{-/-}$ or *Rag1*$^{-/-}$*ICAM-1*$^{-/-}$ mice were intraperitoneally injected with either anti-CD11a blocking antibody or IgG_{2a} control, followed by challenge with IL-33 (500 ng/mouse, intranasally). The frequency and number of eosinophil (Fig. 6 A) and the amount of IL-5 and IL-13 (Fig. 6 B) in the BAL were significantly decreased in *Rag1*$^{-/-}$ mice after anti-CD11a treatment; however, no noticeable effects were observed in *Rag1*$^{-/-}$ *ICAM-1*$^{-/-}$ mice (Fig. 6, A and B). Meanwhile, anti-CD11a treatment decreased the proliferation of lung ILC2s (Fig. 6 C) and thus reduced ILC2 number (Fig. 6 D) in *Rag1*$^{-/-}$ mice, but not in *Rag1*$^{-/-}$*ICAM-1*$^{-/-}$ mice. The production of IL-5 and IL-13 by ILC2 (Fig. 6 E), as well as lung inflammation (Fig. 6 F), were consistently diminished in *Rag1*$^{-/-}$ mice. Administration of anti-CD11a clearly decreased the level of lung ILC2 in *Rag1*$^{-/-}$ mice under steady-state condition (Fig. 6 G). However, no effects were observed for BM iILC2s upon anti-CD11a treatment (Fig. S4, A and B). In line with the observations in mice, anti-human ICAM-1 or anti-human LFA-1 significantly reduced the production of IL-5 and IL-13 from human ILC2s in vitro (Fig. 6 H). These observations indicated that blocking the interaction between ICAM-1 and LFA-1 attenuates ILC2-mediated lung inflammation and their homeostatic maintenance in the periphery.

GATA3 mediates the effect of ICAM-1 on ILC2s

GATA3 is the key transcription factor of ILC2s and regulates the production of ILC2 effector cytokines (Hoyler et al., 2012; Zhong and Zhu, 2017). To investigate the mechanism underlying ICAM-1–mediated ILC2 development and function, the protein level of GATA3 in ILC2s was first evaluated by flow cytometry. Results showed that *ICAM-1*$^{-/-}$ BM iILC2s displayed dramatically reduced GATA3 protein level than WT iILC2, based on two distinct flow cytometric gating strategies (Fig. 7 A and Fig. S5 A). Similar results were observed in lung ILC2s (Fig. S5 B). As expected, the mRNA expression of *Il2ra* and *Cdkn2b*, which are the transcriptional targets of GATA3 (Yagi et al., 2014), in the *ICAM-1*$^{-/-}$ iILC2s

Figure 3. **ICAM-1 deficiency impairs ILC2 function in response to IL-33 challenge. (A and B)** BM cells from WT mice were cultured in the presence of IL-7 (10 ng/ml) with PBS or IL-33 (10 ng/ml) treatment. 2 d later, the expression of ICAM-1 (A) or LFA-1 (B) on BM iILC2s was evaluated by flow cytometry. **(C)** Human PBMCs were cultured in the presence of recombinant human IL-2 (20 ng/ml) and IL-7 (20 ng/ml) with PBS or human IL-33 (20 ng/ml) treatment for 3 d. The MFI levels of ICAM-1 and LFA-1 on human ILC2s (CD45$^+$Lin$^-$CD127$^+$CRTH2$^+$) were evaluated by flow cytometry. **(D)** Equal number of purified lung ILC2s from WT and *ICAM-1*$^{-/-}$ mice were cultured in the presence of IL-2 (10 ng/ml), IL-7 (20 ng/ml), and IL-33 (20 ng/ml) for 3 d, and the amount of IL-5 and IL-13 in the supernatants was evaluated by ELISA. **(E–I)** WT and *ICAM-1*$^{-/-}$ mice were intranasally administered with IL-33 (500 ng/mouse/d) or PBS for three consecutive days (n = 6 for each group). Mice were sacrificed on day 4. **(E)** Representative flow cytometric analysis of ILC2, pregated on CD45$^+$Lin$^-$, and the number of ILC2 in lung from WT and *ICAM-1*$^{-/-}$ mice after PBS or IL-33 treatment. **(F)** Frequencies of IL-5$^+$IL-13$^+$ in lung ILC2s after cell stimulation cocktail treatment for 4 h. IL-33-challenged groups were analyzed. **(G)** The amount of IL-5 and IL-13 in BAL was determined by ELISA. **(H)** The number of eosinophils (CD45$^+$CD11c$^-$ Siglec-F$^+$) in BAL was shown. **(I)** Representative H&E staining of lung sections (bars, 100 µm). Data are representative of two (E–I) to three (A–D) independent experiments. Error bars show mean ± SEM; *, P < 0.05; **, P < 0.01; ***, P < 0.001 by unpaired Student's *t* test. ns, not significant. Numbers within flow plots indicate the percentages of cells gated.

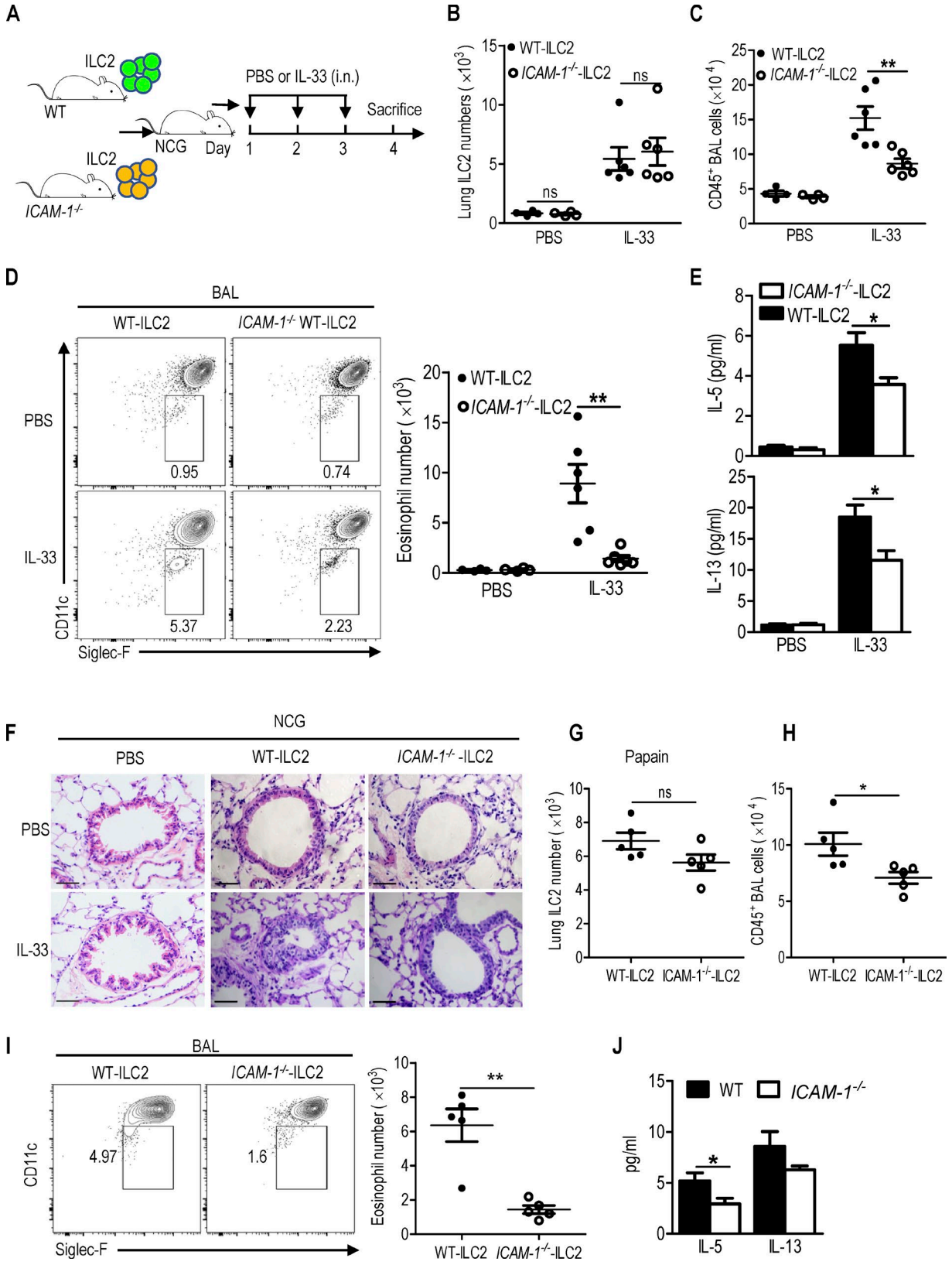

Figure 4. ***ICAM-1*$^{-/-}$ ILC2s fail to induce lung inflammation. (A)** Equal number of lung ILC2s (1.5×10^4) sorted from IL-33-challenged WT or *ICAM-1*$^{-/-}$ mice were intravenously injected into NCG mice, followed by intranasal challenge with IL-33 (n = 6 per group) or PBS (n = 4 per group) for 3 d. Mice were sacrificed 24 h after the last challenge. **(B and C)** The number of ILC2s in lungs (B) and total numbers of CD45$^+$ immune cells in BAL (C) were determined by flow cytometry. **(D)** The frequencies and absolute number of eosinophils in BAL. **(E)** The amount of IL-5 and IL-13 in BAL was measured by ELISA. **(F)** Representative H&E staining of lung sections (bars, 100 µm). **(G–J)** Equal number of lung ILC2s (1.5×10^4) sorted from IL-33–challenged WT or *ICAM-1*$^{-/-}$ mice were intravenously injected into NCG mice, followed by intranasal challenge with papain for 3 d (n = 5 per group). Mice were sacrificed 24 h after the last challenge. The number of

from BM was down-regulated and up-regulated, respectively (Fig. 7 B). Meanwhile, *Il5* and *Il13* mRNA levels in the lung ILC2 of *ICAM-1*$^{-/-}$ mice were significantly lower as compared with those in WT ILC2 (Fig. 7 B). However, no noticeable difference was observed in the mRNA level of *Gata3* between *ICAM-1*$^{-/-}$ and WT ILC2s (Fig. 7 B), suggesting that the dysregulation of GATA3 in *ICAM-1*$^{-/-}$ ILC2s occurred at post-transcriptional level. The expression of other important ILC2 regulators, such as *Rora*, *Est1*, and *Gfi1*, failed to display any differences (Fig. S5 C). Expectedly, ectopic overexpression of GATA3 by retroviral infection clearly rescued the production of IL-13 and IL-5 by *ICAM-1*$^{-/-}$ ILC2s, reaching the level comparable to that in the WT control (Fig. 7 C). These results suggest an essential role of GATA3 in mediating the effects of ICAM-1 on ILC2s.

Binding of ICAM-1 with its ligand LFA-1 could elicit a diverse set of intracellular signaling events involving ERK, p38, and JNK (Hubbard and Rothlein, 2000; Dragoni et al., 2017). ERK signaling was reported to regulate the stability of GATA3 in Th2 cells through ubiquitin-mediated degradation (Yamashita et al., 2005). In addition, ERK signaling could regulate the function of ILC2s (Suzuki et al., 2015). Based on these reports, we proposed that ERK is downstream of ICAM-1 in the regulation of GATA3 stability, and therefore ILC2 function. Intriguingly, flow cytometric analysis revealed that the phosphorylation of Erk1/2 (p-Erk1/2) was significantly lower in *ICAM-1*$^{-/-}$ ILC2s than that in WT ILC2s, both before and after stimulation with PMA (Fig. 7 D). PMA clearly up-regulated GATA3 expression in WT ILC2s (Fig. 7 E) and increased their production of IL-5 and IL-13 (Fig. 7 F). This up-regulation could be abrogated by a specific MEK1/2 inhibitor, U0126, indicating that GATA3 is downstream of the ERK pathway in ILC2s. Moreover, activation of ERK signaling by PMA clearly rescued the defective GATA3 expression (Fig. 7 E) and the IL-5 and IL-13 production (Fig. 7 F) in *ICAM-1*$^{-/-}$ ILC2s. Pretreatment with U0126, however, abrogated these effects (Fig. 7, E and F). Moreover, U0126 treatment did not affect the survival of BM iILC2 (Fig. S5 D). Administration of MG132, a proteasome inhibitor, cancelled the inhibitory effect of U0126 on GATA3 protein, both in WT and *ICAM-1*$^{-/-}$ ILC2s (Fig. 7 G). In contrast to the decreased p-Erk1/2 level, the level of p-p38 did not differ between WT and *ICAM-1*$^{-/-}$ ILC2s (Fig. S5 E). These observations support that ERK signaling regulates the stability of GATA3 protein.

To investigate whether the signaling event induced by ICAM-1 is initiated by its ligand LFA-1, LFA-1 protein was administered to cultured ILC2s. Results showed that LFA-1 significantly enhanced the levels of p-Erk1/2 (Fig. 7 H), GATA3 protein (Fig. 7 I), and the production of IL-5 and IL-13 (Fig. 7 J), in WT ILC2s, but not in *ICAM-1*$^{-/-}$ ILC2s. Pretreatment with U0126 abrogated the effects of LFA-1 on GATA3 (Fig. 7 K) and cytokine production (Fig. 7 L) in ILC2s. These results indicated that ICAM-1, upon interaction with LFA-1, regulates the level of GATA3 protein through ERK signaling.

Discussion

In this study, we demonstrated ICAM-1 as a novel regulator of ILC2. Deficiency of ICAM-1 dramatically impaired the homeostasis and function of ILC2s, which contribute to the remission of lung inflammation. ERK signaling–mediated GATA3 stability explains the potential mechanism.

During the development of CLPs into ILC2s, ICAM-1 and its primary ligand LFA-1 showed a similar dynamic expression pattern. Blocking the interaction between ICAM-1 and LFA-1 suppressed the differentiation of CLP into ILC2, as well as the function of lung ILC2 in airway inflammation models. Exogenous administration of LFA-1 elicited p-Erk1/2 and enhanced the level of GATA3 in WT ILC2s, but not in *ICAM1*$^{-/-}$ ILC2s. These observations indicated that ICAM-1/LFA-1 interaction represents a novel regulator of ILC2 development and function. Interestingly, a recent study showed that β2 integrin, another subunit of the LFA-1 protein, mediated the ILC2 trafficking to the lung in mice (Karta et al., 2018). In our study, comparable levels of ILC2s were observed in NCG recipients of WT and *ICAM1*$^{-/-}$ ILC2s, suggesting that ICAM-1 deficiency may not affect ILC2 migration to the lungs. The role of ICAM-1 in the migration of ILC2s, however, requires further investigation.

As ILC2 development occurs in the BM of adult mice, whereas ICAM-1 can be expressed on a variety of stroma cells including endothelial, fibroblastic, and epithelial cells (Ramos et al., 2014), it is plausible that the impaired ILC2s in *ICAM-1*$^{-/-}$ mice may be caused by the BM microenvironment. However, adoptive transfer of CLPs into NCG mice revealed that *ICAM-1*$^{-/-}$ CLPs failed to differentiate into ILC2s efficiently, indicating that ICAM-1 regulates the development of ILC2 in a cell-intrinsic manner. Defective differentiation of *ICAM-1*$^{-/-}$ CLPs into ILC2 in vitro further supports this possibility. Furthermore, blocking antibodies against LFA-1 or ICAM-1 diminished the generation of ILC2 from WT CLP, indicating that ICAM-1/LFA-1 signaling could regulate the development of iILC2 in BM. Intriguingly, neither the OP9-DL1 cell line nor BM stroma cells expressed LFA-1, while CLPs did express relatively higher levels of LFA-1. It is therefore possible that LFA-1 signals, provided by CLP or its downstream of ILC2 progenitors, enhance the differentiation of CLP into ILC2 through interaction with ICAM-1. Stroma cells may provide other essential signals for ILC2 generation. Meanwhile, the expression of ICAM-1 on ILC2s was induced by IL-33 stimulation. It is also possible that stroma cells from the tissue microenvironment secretes IL-33 under certain circumstances, which leads to up-regulation of ICAM-1 and the generation of ILC2s.

The deficiency of ICAM-1 caused systematical reduction of ILC2 in multiple peripheral tissues. As ILC2s are tissue resident cells and they are maintained by self-renewal in the peripheral tissues under physiological condition, and they do not migrate in circulation even under inflammation (Gasteiger et al., 2015; Moro et al., 2016), the reduced number of ILC2s in the periphery from *ICAM-1*$^{-/-}$ mice may not necessarily be caused by their

Lung ILC2 (G), CD45^{+} BAL cells (H), and levels of eosinophils in BAL (I) were determined by flow cytometry. The amount of IL-5 and IL-13 in BAL was measured by ELISA (J). Data are representative of two independent experiments. Error bars show mean ± SEM; *, $P < 0.05$; **, $P < 0.01$. ns, not significant. Numbers within flow plots indicate the percentages of cells gated.

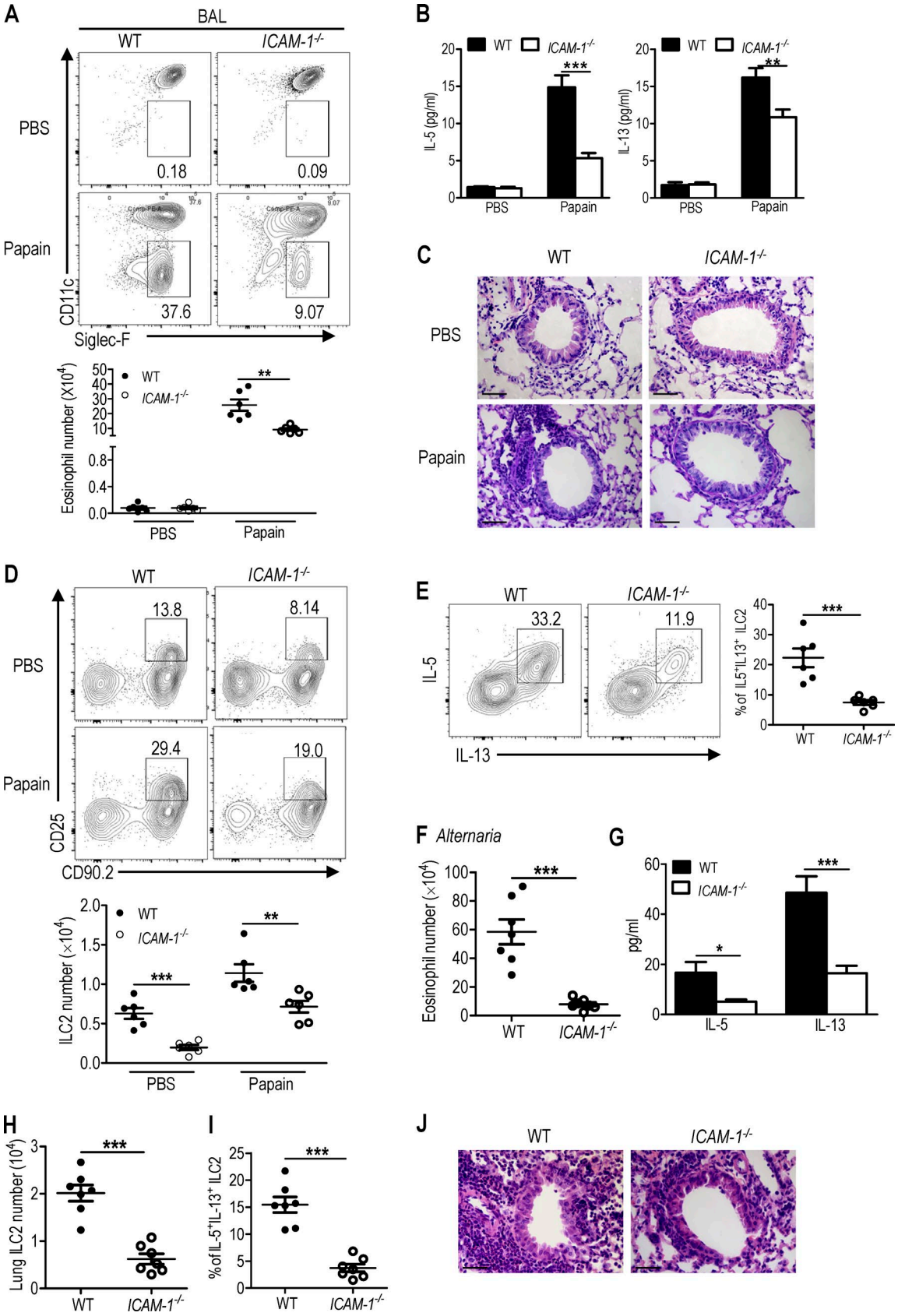

Figure 5. **ICAM-1 deficiency attenuates papain and *A. alternata*–induced lung inflammation. (A–E)** WT and *ICAM-1*$^{-/-}$ mice were intranasally administered with papain or PBS for 5 d (n = 6 for each group). Mice were sacrificed 24 h after the last treatment. **(A)** The frequencies and number of eosinophils in BAL were evaluated by flow cytometry. **(B)** The amount of IL-5 and IL-13 in BAL was measured by ELISA. **(C)** Representative lung histology by H&E staining (bars, 100 µm). **(D)** The frequencies and number of lung ILC2s were determined by flow cytometry. **(E)** Flow cytometric analysis of frequencies of IL-5$^+$IL-13$^+$ in lung ILC2s

developmental defect in the BM. Administration of anti-LFA-1/CD11a led to a clear reduction in the level of lung ILC2 under both steady-state and IL-33 challenge, even though no clear effects were observed for BM iILC2 based on the protocol we used. These results raise the possibility that ICAM-1/LFA-1 signaling could directly regulate the homeostasis of tissue resident ILC2. No effect on the level of BM iILC2 upon anti-LFA-1/CD11a treatment may be caused by lower amount of antibody available in the BM, when compared with the peripheral tissues. Deficiency of ICAM-1 or administration of anti-CD11a decreased the number of lung ILC2s, whereas the number of lung ILC2 was comparable between *ICAM-1*$^{-/-}$ and WT controls after transfer into NCG mice (Fig. 4 B). This may be due to that *ICAM-1*$^{-/-}$ and WT mice were pretreated with IL-33 and ILC2s were expanded before injecting into NCG mice, which may make them less responsive to IL-33 challenge after transfer into NCG mice.

Although ICAM-1 deficiency causes attenuation of airway inflammation in several models we used, IL-33 administration appears most pronounced. As IL-33 secreted from airway epithelial cells mediates the effects of papain and other allergens on ILC2 responses during allergic inflammation (Oboki et al., 2010; Kamijo et al., 2013), it is possible that the difference in the sensitivity of distinct models may be attributed to the available amount of IL-33 in the lung. IL-33 challenge may provide more IL-33 than papain or other allergens do; therefore, it elicited a stronger airway inflammation. Moreover, IL-33 induces the expression of ICAM-1, which may further amplify its effect on ILC2 function.

There is some evidence for the interaction between ICAM-1 and LFA-1 (CD18/CD11a) participating in the pathology of experimental allergic diseases such as asthma (Wegner et al., 1990; Nakao et al., 1994; Iwamoto and Nakao, 1995), which was partly attributed to impaired Th2 responses, though different groups have obtained contrasting observations (Nakajima et al., 1994; Salomon and Bluestone, 1998). In this study, it was found that both Th2 and ILC2 responses were impaired in *ICAM-1*$^{-/-}$ mice in OVA-induced asthma mouse model, suggesting that ICAM-1 regulates the function of both Th2 and ILC2. Compared with *Rag1*$^{-/-}$ control mice, *ICAM-1*$^{-/-}$*Rag1*$^{-/-}$ mice consistently displayed impaired ILC2 function and remission of lung inflammation in papain model. Furthermore, anti-CD11a blocking antibodies apparently reduced the number of lung ILC2s, as well as their cytokine production, in *Rag1*$^{-/-}$ mice, but not in *ICAM-1*$^{-/-}$ *Rag1*$^{-/-}$ mice. These results indicated that the regulation of ILC2s by ICAM-1 is independent of CD4 T cells.

GATA3 is a key regulator of ILC2 development, maintenance, and function (Hoyler et al., 2012; Mjösberg et al., 2012). Remarkably reduced levels of GATA3 protein were observed in *ICAM-1*$^{-/-}$ ILC2s, compared with WT ILC2s. The ectopic overexpression of GATA3 rescued the functional defects of *ICAM-1*$^{-/-}$ ILC2s, suggesting that GATA3 mediates the regulatory effects of ICAM-1 on ILC2. Interestingly, the mRNA expression of *Gata3* was not affected by the absence of ICAM-1, indicating that ICAM-1 regulates GATA3 at the post-transcriptional level. The ERK signaling pathway regulates the protein level of GATA3 (Yamashita et al., 2005). Inhibition of protein degradation by proteasome inhibitor MG132 abrogated the effect of U0126 on GATA3 protein, suggesting that GATA3 stability in ILC2s is controlled by ERK signaling. This mechanism has also been reported in Th2 cells (Yamashita et al., 2005). Due to the limited number of ILC2s, we did not evaluate GATA3 ubiquitination and degradation. Considering that CD25 is a downstream target of GATA3 (Yagi et al., 2014), use of CD25 as one of the markers to define ILC2 may not be appropriate for our study; therefore, we used alternative flow cytometric gating strategies (independent of CD25) to confirm the reduction of ILC2 in both BM and lung.

In conclusion, our study demonstrated that ICAM-1 is required for both development and function of ILC2s. We demonstrated that the ERK signaling pathway is impaired in *ICAM-1*$^{-/-}$ ILC2s, leading to a decreased level of GATA3 protein and diminished type 2 cytokine production in response to allergens. Blocking the interaction between ICAM-1 and LFA-1 impairs the function of ILC2s and relieves lung inflammation. Our findings provide new avenues for designing novel therapeutics that target ILC2s to treat asthma and allergic diseases.

Materials and methods

Mice

ICAM-1$^{-/-}$ mice (B6.129S4-Icam1^{tm1Jcgr}/J, 002867) were purchased from The Jackson Laboratory. *Rag-1*$^{-/-}$ mice (B6.129S7-Rag1^{tm1Mom}/JNju) and NCG mice (NOD-Prkdc^{em26Cd52}Il2rg^{em26Cd22}/Nju) were purchased from Nanjing Biomedical Research Institute of Nanjing University. C57B/L6 mice were purchased from Guangdong Medical Laboratory Animal Center. C57B/L6-Ly5.1 (CD45.1) mice were provided by H. Wang from Institut Pasteur of Shanghai, Chinese Academy of Sciences. All mice were housed and maintained according to Sun Yat-sen University guidelines and used at the age of 8–10 wk. All mouse experimental procedures were approved by the Institutional Animal Care and Use Committee of Sun Yat-sen University.

Lung inflammation mouse models

For IL-33–induced airway inflammation, recombinant mouse IL-33 (500 ng/mouse; BioLegend), or PBS was intranasally administered into mice on days 1, 2, and 3 (Maazi et al., 2015). 24 h after the final treatment, mice were sacrificed and samples were collected. For induction of papain-induced acute type 2 airway inflammation (Monticelli et al., 2016), mice were anesthetized, followed by intranasal administration with papain (20 µg papain

after cell stimulation cocktail treatment for 4 h. Papain treated groups were analyzed. **(F–J)** WT and *ICAM-1*$^{-/-}$ mice were intranasally challenged with extract of *A. alternata* for 4 d (n = 7). Mice were sacrificed 24 h after the last challenge. **(F)** The number of eosinophils in BAL was evaluated by flow cytometry. **(G)** The amount of IL-5 and IL-13 in BAL was measured by ELISA. **(H)** Total number of ILC2 in lung after *A. alternata* treatment. **(I)** The frequencies of IL-5$^+$IL-13$^+$ in lung ILC2s after cell stimulation cocktail treatment for 4 h. **(J)** Representative H&E staining of lung sections in *A. alternata*–treated groups (bars, 100 µm). Data are representative of two independent experiments. Error bars show mean ± SEM; **, P < 0.01; ***, P < 0.001 by unpaired Student's *t* test. Numbers within flow plots indicate the percentages of cells gated.

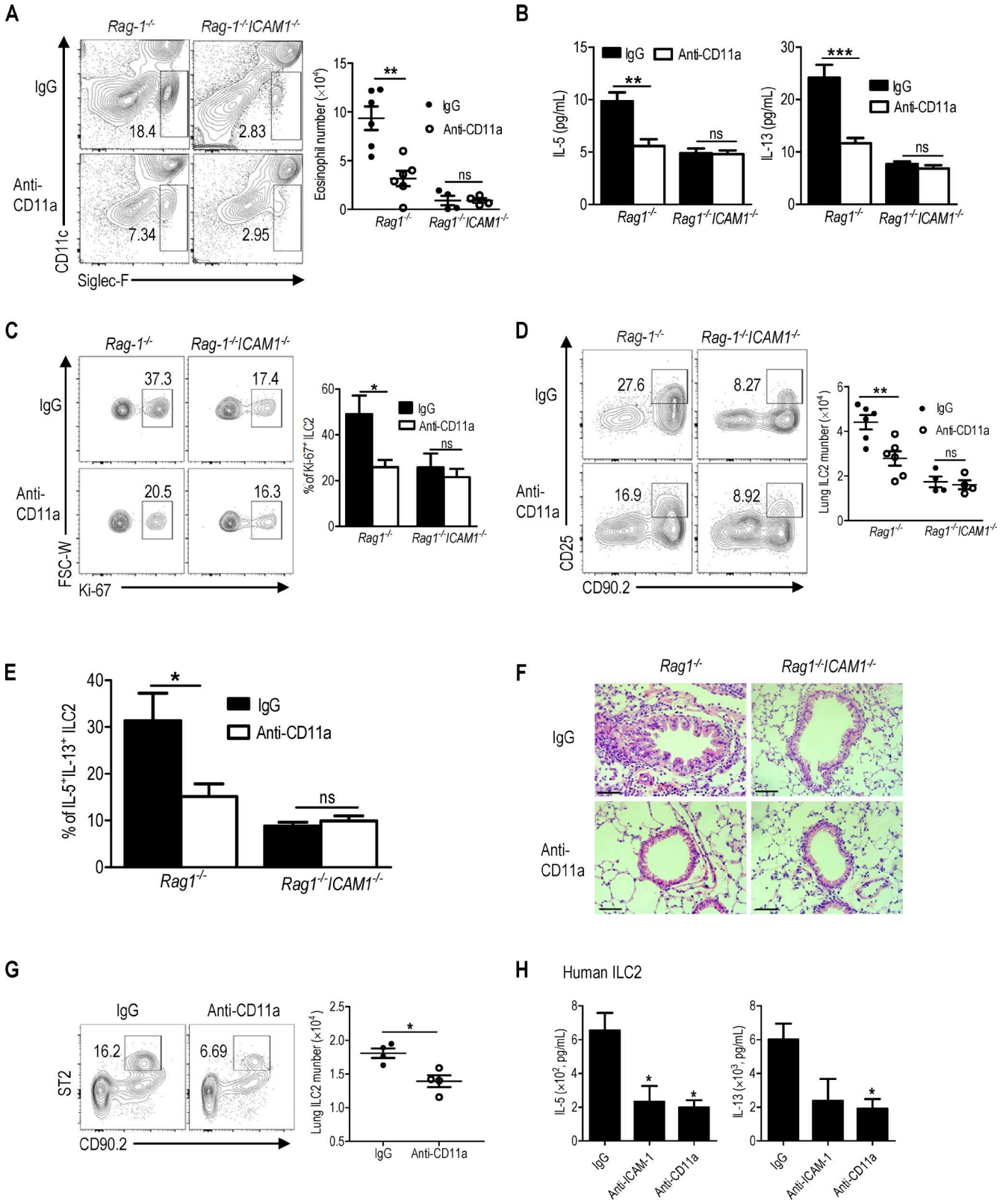

Figure 6. **Blocking ICAM-1 and LFA-1 interaction attenuates IL-33–induced lung inflammation.** *Rag1*$^{-/-}$ and *Rag*$^{-/-}$*ICAM-1*$^{-/-}$ mice were injected intraperitoneally with anti-mouse CD11a (100 µg/mouse) or IgG (100 µg/mouse) on day 0, followed by intranasally challenge with IL-33 (500 ng/mouse/d) for three consecutive days (n = 4 or 6 per group). Mice were sacrificed on day 4 after 24 h of the last challenge. **(A)** Representative flow plots of eosinophils, pregated on CD45^{+} cells and their numbers were shown. **(B)** The amount of IL-5 and IL-13 in BAL was determined by ELISA. **(C)** The proliferation of lung ILC2s was determined by Ki-67 staining (n = 3–4). **(D)** The frequencies and absolute number of ILC2s in lung. **(E)** Frequencies of IL-5^{+}IL-13^{+} in ILC2s from lung were shown. Cells were pretreated with stimulation cocktail for 4 h before flow cytometric analysis. **(F)** Representative lung histology by H&E staining (bars, 100 µm). **(G)** *Rag1*$^{-/-}$ mice (n = 4 per group) were injected intraperitoneally with anti-mouse CD11a (100 µg/mouse) or IgG (100 µg/mouse) antibodies on day 0. Mice were sacrificed on

in 40 µl PBS, daily) or PBS for five consecutive days. BAL fluid and lungs were harvested for analysis on day 6. For *A. alternata*–induced lung inflammation, mice were intranasally administrated with 100 µg *A. alternata* (Greerlabs) in 40 µl PBS for four consecutive days as previously described (Maazi et al., 2015). Mice were sacrificed 24 h after the last challenge, and BAL fluid and lungs were collected for analysis. For OVA-induced chronic allergic inflammation (Shi et al., 2014), mice were intraperitoneally sensitized with 100 µg OVA (Grade V, emulsified in 10 mg of aluminum hydroxide; Sigma-Aldrich) on days 0 and 7, followed by intranasal instillation with OVA (100 µg in 40 µl PBS) on days 14, 15, 16, and 17. Mice were sacrificed for analysis 24 h after the last challenge.

Isolation of cells from tissue

BM cells were obtained by flushing femurs and tibias with a syringe containing RPMI-1640 media. Red blood cells were lysed with ACK buffer. To isolate cells from BAL fluid and lung tissue, we flushed the lungs with 0.8 ml of cold PBS twice via a thin tube inserted into a cut made in the trachea as described (Monticelli et al., 2016). Then, lungs were perfused with 10 ml cold PBS through the right ventricle of the heart before removal. Lung lobes were cut into small pieces with scissors and digested with 0.5 mg/ml collagenase type I (Invitrogen) in RPMI-1640 media with 10% FBS (Biological Industries) and 1% penicillin-streptomycin (Gibco) for 1 h at 37°C with continuous agitation in an incubator. The crude suspensions were further filtered through 70-µm cell strainers and the remaining red blood cells were lysed with ammonium-chloride-potassium (ACK) buffer. Leukocytes were obtained by a 40/80% Percoll (GE Healthcare) gradient. Splenocytes and mLN cells were obtained by mechanical disruption on 70-µm cell strainers. Red blood cells were lysed with ACK buffer. Isolation of cells from large and small intestine was performed by digestion in 0.5 mg/ml collagenase I and 5 U/ml DNase for 40 min after removal of intestinal epithelial cells as described (Seehus et al., 2015). Leukocytes from lamina propria were enriched by a 40/80% Percoll gradient. Cell suspensions from all tissues were filtered through 70-µm cell strainers before subsequent use.

Human PBMC isolation

This study was approved by the Ethics Review Board of Sun Yat-sen University and written informed consent was provided by the participants. Human peripheral blood mononuclear cells (PBMCs) from fresh blood samples were isolated by Ficoll centrifugation as described earlier (Qin et al., 2013). PBMCs were washed and resuspended in PBS containing 1% FBS on ice before subsequent use.

Flow cytometric analysis and sorting

Single-cell suspensions were incubated with an unlabeled purified anti-Fc receptor blocking antibody (anti-CD16/CD32) before staining with fluorochrome-conjugated antibodies. A cell viability dye (The live/dead fixable far-red dead cell stain kit; Invitrogen) was used to exclude dead cells from subsequent analysis. Cells were acquired on an LSRFortessa flow cytometer (BD Bioscience), and data were analyzed with the FlowJo V10.0.7 (FlowJo). The fraction of labeled cells was analyzed with a minimum 100,000 events. For staining of transcription factor, cells were stained with antibodies to surface antigens, fixed and permeabilized according to the manufacturer's instructions (Foxp3/Transcription Factor Staining Buffer Set; eBioscience). For measurement of intracellular cytokine expression, cells were isolated ex vivo and stimulated in complete RPMI-640 media + 10% FBS with 50 ng/ml PMA (Sigma-Aldrich), 1 µg/ml ionomycin (Sigma-Aldrich), and 1 µg/ml brefeldin A (eBioscience) for 4 h. Cells were subsequently surface-stained, fixed, and permeabilized using an intracellular fixation and permeability kit (eBioscience), and stained with indicated cytokines. For the flow cytometric sorting, a BD FACSAriaIII cell sorter (BD Bioscience) was used. Antibodies used are listed in Table S1. For mouse ILC2 sorting, cells were initially depleted of T, B, myeloid, and erythroid lineages by labeling with biotin-conjugated anti-CD3, anti-CD45R/B220, anti-CD11b, anti-Ly6G, and anti-Erythroid marker (TER-119), followed by Streptavidin-paramagnetic particles (BD Bioscience) according to manufacturer's instructions. The left cells then were stained with the specific fluorochrome-conjugated antibodies (BM iILC2s: $CD45^+Lin^-Sca1^{high}CD127^+CD25^+$; Lung ILC2s: $CD45^+Lin^-CD90.2^+CD25^+$) and sorted with Aria III (BD Bioscience). For human ILC2 sorting, human PBMCs were first depleted of T cells, B cells, NK cells, myeloid cells, granulocytes, and red blood cells by labeling with biotin-conjugated anti-CD2, anti-CD3, anti-CD10, anti-CD11b, anti-CD14, anti-CD16, anti-CD19, anti-CD56, anti-CD123, and anti-CD235a, then magnetic beads that, when placed in a magnetic field, leave lineage negative cells untouched and free in solution. Then, the collected lineage negative cells were stained with the specific fluorochrome-conjugated antibodies for ILC2s ($CD45^+Lin^-CD127^+CRTH2^+$). All the cells were sorted with a purity ≥95%.

Cell adoptive transfer into NCG mice

For generation of BM chimeras: CLPs from *ICAM-1*$^{-/-}$ mice ($CD45.2^+$) and C57B/L6-Ly5.1/Ly5.2 mice ($CD45.1/2^+$) were sorted (1.5×10^4) and mixed at 1:1 ratio, followed by adoptive transfer into NCG mice ($CD45.1^+$). Mice were sacrificed and analyzed 3 wk later. For ILC2 transfer experiment, lung ILC2s (1.5×10^4 cells/mouse) were sorted from IL-33 challenged *ICAM-1*$^{-/-}$ and WT controls, followed by intravenous injection into NCG mice, respectively. Mice were then challenged with IL-33 (intranasally) for three consecutive days to induce lung inflammation. Mice were sacrificed and analyzed 24 h after the last challenge.

day 3. Representative flow plots of lung ILC2, pregated on $CD45^+Lin^-$ cells and the number of lung ILC2 was evaluated by flow cytometry. **(H)** Human ILC2s were treated with IgG, anti-human ICAM-1 or anti-human CD11a in the presence of IL-2 (20 ng/ml), IL-7 (20 ng/ml), and IL-33 (20 ng/ml) for 3 d. The amount of IL-5 and IL-13 in the supernatant was determined by ELISA. Data are representative of two (A–G) to three (H) independent experiments. Error bars show mean ± SEM; *, $P < 0.05$; **, $P < 0.01$; ***, $P < 0.001$ by unpaired Student's *t* test. ns, not significant. Numbers within flow plots indicate the percentages of cells gated.

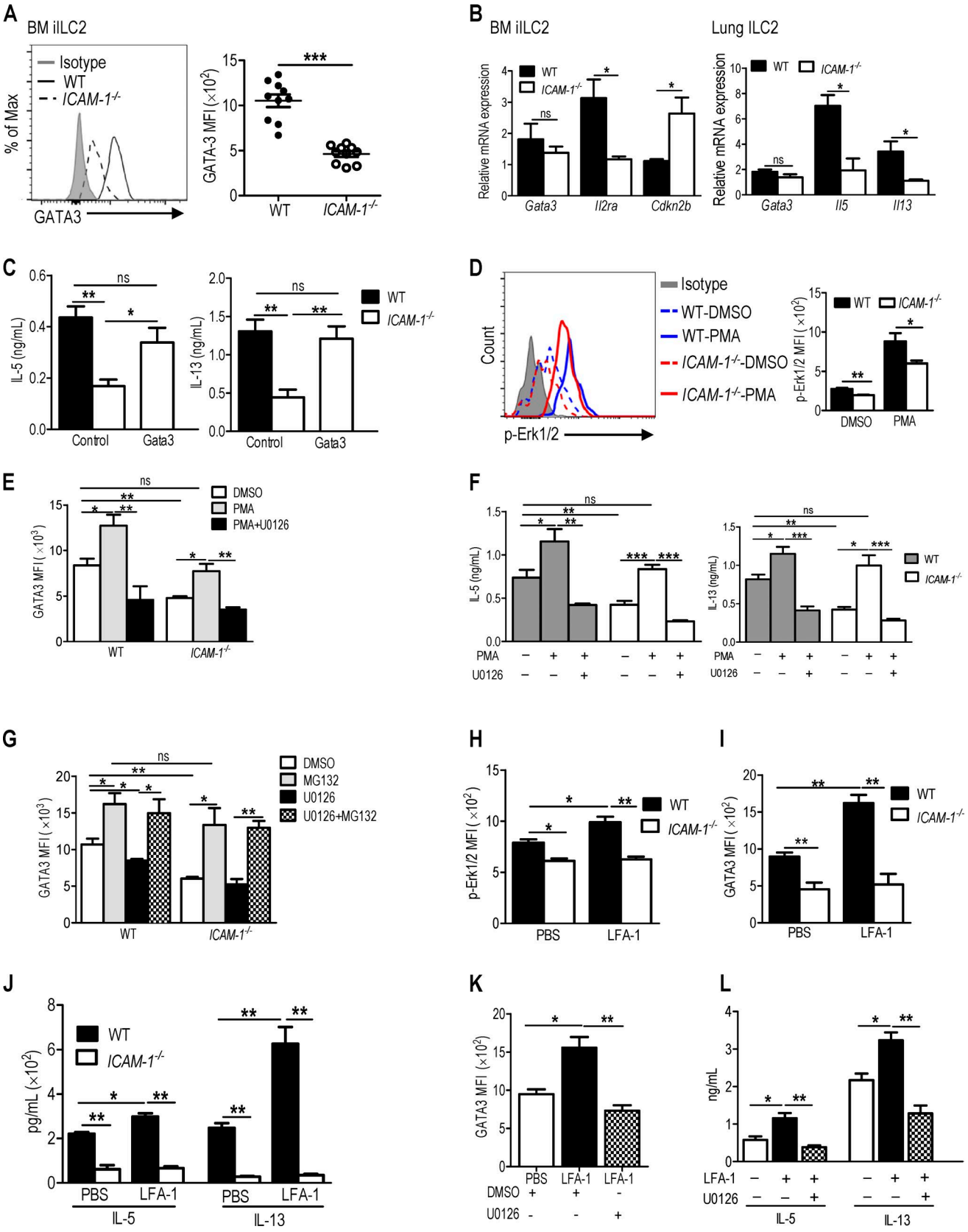

Figure 7. **GATA3 mediates the effect of ICAM-1 on ILC2s. (A)** Flow cytometric analysis of GATA3 expression in BM iILC2s, pregated on CD45⁺Lin⁻Sca1^{high}C-D127⁺CD25⁺ (n = 10). **(B)** The mRNA expression of *Gata3*, *Il2ra* and *Cdkn2b* in BM iILC2s (left) or *Il5* and *Il13* in lung ILC2s (right) from WT and *ICAM-1*$^{-/-}$ mice was evaluated by qRT-PCR. **(C)** BM iILC2s were infected with retrovirus expressing GATA3 or vector control in the presence of 10 ng/ml of IL-2, IL-7, and IL-33 for 3 d. The amount of IL-5 and IL-13 in the culture supernatants was measured by ELISA. **(D)** Representative flow analysis of the levels of p-Erk1/2 in BM iILC2 from

ILC2 cell culture

For in vitro ILC2 differentiation, we followed the protocol as described earlier (Seehus et al., 2015; Koga et al., 2018,). In brief, purified CLPs (3,000 cells/well) were co-cultured with mitomycin-c treated OP9-DL1 cell line in the presence of IL-7 (10 or 20 ng/ml), with or without IL-33 (20 ng/ml) in 96-well plates. For in vitro B cell differentiation, the same number of CLPs were co-cultured with mitomycin-c treated OP9 cell line in the presence of IL-7 (10 ng/ml), SCF (50 ng/ml), and Flt3L (5 ng/ml). In both co-culture systems, mediums were half changed every 3 d and ILC2 ($Lin^-CD45^+ICOS^+CD25^+$) or B cells ($CD45^+CD19^+B220^+$) were analyzed on day 9 or 10. For ILC2 function analysis in vitro, lung ILC2s were cultured in 96-well plates with a density of 5×10^3 per well, in the presence of mouse IL-33 (20 ng/ml), IL-2 (10 ng/ml), and IL-7 (20 ng/ml) for 72 h. Then, the amount of cytokines in culture supernatants was measured by ELISA. Sorted BM iILC2s (5×10^3 – 10^4 cells/well) were cultured in the presence of IL-33 (100 ng/ml), IL-2 (10 ng/ml), and IL-7 (20 ng/ml), unless otherwise indicated. Mediums were half changed every 3 d and analyzed at indicated time. To evaluate human ILC2 function, human ILC2s (5,000 cells/well) were cultured in 96-well plates in the presence of recombinant human IL-33 (20 ng/ml), IL-7 (20 ng/ml), and IL-2 (20 ng/ml) for 3 d and the supernatants were collected for IL-5 and IL-13 measurement.

Quantitative real-time PCR (qRT-PCR)

Total RNA from purified ILC2s was extracted using TRIzol (Invitrogen) and reverse transcribed with a synthesis kit (Takara), and gene expression was analyzed by qRT-PCR with SYBR green chemistry (Takara). The sequences of primer used are listed in Table S2.

Retroviral transduction

Retroviral supernatant preparation and viral transduction were performed as described previously (Yang et al., 2013). For retroviral transduction of ILC2, BM iILC2s were sorted from WT and *ICAM-1*$^{-/-}$ mice and were cultured overnight with 10 ng/ml of IL-2, IL-7, and IL-33. The next day, cells were resuspended in retroviral supernatant supplemented with the above cytokines as well as 8 µg/ml polybrene, centrifuged at 1,400 *g* for 2 h at 32°C, then cultured at 37°C for another 6 h. Cells were subsequently washed with 1640 medium and cultured in fresh complete medium with 10 ng/ml of IL-2, IL-7, and IL-33. 3 d later, the supernatants were collected for the analysis of IL-5 and IL-13 by ELISA.

ELISA

BAL fluid from lung inflammation mouse models or supernatants from cultured ILC2 were collected. The amounts of IL-13 and IL-5 were measured by ELISA, following the manufacturer's instructions (eBioscience).

CLP homing assay

CLP homing assay was performed as described (Zhang et al., 2006). BM cells from WT or *ICAM-1*$^{-/-}$ mice were labeled with CFSE (Invitrogen), followed by intravenously transferred into lethally irradiated WT mice (10^7 cells per mouse). The number of donor-derived $CFSE^+$ CLPs were evaluated by flow cytometry after transfer for 18 h.

DSS-induced colitis model

Weight matched WT and *ICAM-1*$^{-/-}$ mice were given 2.5% DSS (MP Biomedicals) in drinking water for 7 d. Mice were monitored daily for weight loss, stool consistency, and hematochezia. Mice were sacrificed on day 7 and the function of ILC1 and ILC3 in lamina propria from colon was evaluated by flow cytometry.

Statistical analysis

All data are derived from two to four independent experiments. Statistical analysis was performed with GraphPad Prism 5.0 software (GraphPad Software, La Jolla, CA). Results show mean ± SEMs, and statistical significance was determined by a two-tailed unpaired Student's *t* test or one-way ANOVA with Bonferroni post-test. Differences were considered significant when P value < 0.05.

Online supplemental material

Fig. S1 shows the gating strategy for ILC2 and their progenitors; LFA-1 expression during ILC2 development, as well as on $CD4^+$ T cells; the number of BM iILC2 by using an independent gating strategy; the loss of T cells, B cells, and ILC2s in NCG mice; the effect of ICAM-1 deficiency on the CLP homing; the differentiation of CLPs into ILC2s or B cells in vitro; and the survival and proliferation of *ICAM-1*$^{-/-}$ and WT iILC2s in vitro. Fig. S2 shows another gating strategy for lung ILC2, human ILC2 analysis, and ICAM-1 and LFA-1 expression on human ILC2s; the impaired function of *ICAM-1*$^{-/-}$ BM iILC2s after in vitro culture; and the effect of ICAM-1 deficiency on the function of ILC1 and ILC3 by using a DSS-induced colitis model. Fig. S3 demonstrates the effect of ICAM-1 on ILC2-induced lung inflammation is independent of Th2 response. Fig. S4 shows that anti-CD11a administration does not impact the level of BM iILC2s. Fig. S5 demonstrates the decreased GATA3 protein level in *ICAM-1*$^{-/-}$ ILC2s, and the effect of ICAM-1 deficiency on the mRNA expression of *Rora*, *Ets1*, and *Gfi1* in ILC2s, and the influence of U0126 on the survival of iILC2s, as well as the level of p-p38 between WT and *ICAM-1*$^{-/-}$

WT (blue) and *ICAM-1*$^{-/-}$ (red) after DMSO or PMA treatment for 15 min, and the MFI of p-Erk1/2 were shown. **(E)** Flow cytometric analysis of GATA3 MFI in BM iILC2s cultured in the presence of IL-2, IL-7, and IL-33 (20 ng/ml) with the indicated treatments for 12 h. **(F)** The amount of IL-5 and IL-13 in the supernatants of 24 h culture from (E) was measured by ELISA. **(G)** BM cells from WT and *ICAM-1*$^{-/-}$ mice were treated with MG132 (20 µM) and/or U0126 (20 µM) in the presence of 10 ng/ml of IL7 and IL-33 for 6 h. The levels of GATA3 in iILC2 were determined by flow cytometry. **(H–J)** BM iILC2s from WT and *ICAM-1*$^{-/-}$ mice were treated with PBS or LFA-1 protein (0.4 µg/ml) in the presence of IL-2 (10 ng/ml), IL-7 (10 ng/ml), and IL-33 (10 ng/ml). The levels of p-Erk1/2 in ILC2 were measured by flow cytometry after 2 h treatment (H), GATA3 expression in ILC2s was determined by flow cytometry on day 3 (I), and cytokine production by ILC2s was measured by ELISA on day 3 (J). **(K)** Expression of GATA3 in BM iILC2s after the indicated treatment for 24 h. LFA-1 protein: 0.4 µg/ml; U0126: 20 µM; DMSO: 0.1%. **(L)** The amount of IL-5 and IL-13 in culture supernatants from K. Data are representative of three independent experiments. Error bars show mean ± SEM; *, P < 0.05; **, P < 0.01; ***, P < 0.001 by unpaired Student's *t* test (A–D and H–J) or one-way ANOVA with Bonferroni post-test (E–G and K and L). ns, not significant.

iILC2s. Table S1 shows the antibodies used in this study. Table S2 shows primer sequences used for qRT-PCR.

Acknowledgments

We would like to thank Juan Carlos Zúñiga-Pflücker at Sunnybrook Research Institute for providing OP9-DL1 cell line.

This work was supported by the following grants to J. Zhou: Guangdong Province Universities and Colleges Pearl River Scholar Funded Scheme (GDUPS, 2014), National Natural Science Foundation of China (grants 91542112, 81571520, 81771665, and 81742002), the Leading Talents Cultivated by "Thousand-Hundred-Ten" Program of Guangdong Province, 111 Project (grant B12003), Science and Technology Program of Guangzhou (grant 201707010452), and Natural Science Foundation of Guangdong Province (grant 2017B030311014). It was also supported by the Recruitment Program for Foreign Experts (The Thousand Talents Plan, grant WQ20144400204 to D.I. Gabrilovich), and the Leading Talents of Guangdong Province Program. Start-up Fund for High-level Talents of Sun Yat-sen University (D.I. Gabrilovich), the National Key Research and Development Program of China (grant 2016YFA0502202 to H.-K. Wang), the National Natural Science Foundation of China (grant 31570886 to H.-K. Wang), and China Postdoctoral Science Foundation (2017M612809 to A.-H. Lei).

The authors declare no competing financial interests.

Author contributions: A.-H. Lei and Q. Xiao designed and performed most experiments and analyzed the data. G.-Y. Liu, K. Shi, Q. Yang, X. Li, Y.-F. Liu, and Y.-J. Guan. participated in the experiments. H.-K. Wang, W.-P. Cai, and D.I. Gabrilovich participated in experiments design, edited the manuscript. J. Zhou conceptualized, supervised, interpreted the experiments and wrote the paper.

Submitted: 30 December 2017
Revised: 2 May 2018
Accepted: 3 July 2018

References

Antignano, F., M. Braam, M.R. Hughes, A.L. Chenery, K. Burrows, M.J. Gold, M.J. Oudhoff, D. Rattray, T.Y. Halim, A. Cait, et al. 2016. G9a regulates group 2 innate lymphoid cell development by repressing the group 3 innate lymphoid cell program. *J. Exp. Med.* 213:1153–1162. https://doi.org/10.1084/jem.20151646

Artis, D., and H. Spits. 2015. The biology of innate lymphoid cells. *Nature.* 517:293–301. https://doi.org/10.1038/nature14189

Bendjelloul, F., P. Malý, V. Mandys, M. Jirkovská, L. Prokesová, L. Tucková, and H. Tlaskalová-Hogenová. 2000. Intercellular adhesion molecule-1 (ICAM-1) deficiency protects mice against severe forms of experimentally induced colitis. *Clin. Exp. Immunol.* 119:57–63. https://doi.org/10.1046/j.1365-2249.2000.01090.x

Bijanzadeh, M., N.B. Ramachandra, P.A. Mahesh, M.R. Savitha, G.S. Vijayakumar, P. Kumar, B.S. Manjunath, and B.S. Jayaraj. 2009. Soluble intercellular adhesion molecule-1 and E-selectin in patients with asthma exacerbation. *Hai.* 187:315–320.

Brestoff, J.R., B.S. Kim, S.A. Saenz, R.R. Stine, L.A. Monticelli, G.F. Sonnenberg, J.J. Thome, D.L. Farber, K. Lutfy, P. Seale, and D. Artis. 2015. Group 2 innate lymphoid cells promote beiging of white adipose tissue and limit obesity. *Nature.* 519:242–246. https://doi.org/10.1038/nature14115

Cao, Z., T. Ye, Y. Sun, G. Ji, K. Shido, Y. Chen, L. Luo, F. Na, X. Li, Z. Huang, et al. 2017. Targeting the vascular and perivascular niches as a regenerative therapy for lung and liver fibrosis. *Sci. Transl. Med.* 9:eaai8710. https://doi.org/10.1126/scitranslmed.aai8710

Chang, J.E., T.A. Doherty, R. Baum, and D. Broide. 2014. Prostaglandin D2 regulates human type 2 innate lymphoid cell chemotaxis. *J. Allergy Clin. Immunol.* 133:899–901.e3. https://doi.org/10.1016/j.jaci.2013.09.020

De Rose, V., G. Rolla, C. Bucca, P. Ghio, M. Bertoletti, P. Baderna, and E. Pozzi. 1994. Intercellular adhesion molecule-1 is upregulated on peripheral blood T lymphocyte subsets in dual asthmatic responders. *J. Clin. Invest.* 94:1840–1845. https://doi.org/10.1172/JCI117533

Dragoni, S., N. Hudson, B.A. Kenny, T. Burgoyne, J.A. McKenzie, Y. Gill, R. Blaber, C.E. Futter, P. Adamson, J. Greenwood, and P. Turowski. 2017. Endothelial MAPKs Direct ICAM-1 Signaling to Divergent Inflammatory Functions. *J. Immunol.* 198:4074–4085. https://doi.org/10.4049/jimmunol.1600823

Dustin, M.L., T.G. Bivona, and M.R. Philips. 2004. Membranes as messengers in T cell adhesion signaling. *Nat. Immunol.* 5:363–372. https://doi.org/10.1038/ni1057

Ebbo, M., A. Crinier, F. Vély, and E. Vivier. 2017. Innate lymphoid cells: major players in inflammatory diseases. *Nat. Rev. Immunol.* 17:665–678. https://doi.org/10.1038/nri.2017.86

Fine, J.S., and A.M. Kruisbeek. 1991. The role of LFA-1/ICAM-1 interactions during murine T lymphocyte development. *J. Immunol.* 147:2852–2859.

Furusho, S., S. Myou, M. Fujimura, T. Kita, M. Yasui, K. Kasahara, S. Nakao, K. Takehara, and S. Sato. 2006. Role of intercellular adhesion molecule-1 in a murine model of toluene diisocyanate-induced asthma. *Clin. Exp. Allergy.* 36:1294–1302. https://doi.org/10.1111/j.1365-2222.2006.02568.x

Gasteiger, G., X. Fan, S. Dikiy, S.Y. Lee, and A.Y. Rudensky. 2015. Tissue residency of innate lymphoid cells in lymphoid and nonlymphoid organs. *Science.* 350:981–985. https://doi.org/10.1126/science.aac9593

Geiger, T.L., M.C. Abt, G. Gasteiger, M.A. Firth, M.H. O'Connor, C.D. Geary, T.E. O'Sullivan, M.R. van den Brink, E.G. Pamer, A.M. Hanash, and J.C. Sun. 2014. Nfil3 is crucial for development of innate lymphoid cells and host protection against intestinal pathogens. *J. Exp. Med.* 211:1723–1731. https://doi.org/10.1084/jem.20140212

Halim, T.Y., R.H. Krauss, A.C. Sun, and F. Takei. 2012a. Lung natural helper cells are a critical source of Th2 cell-type cytokines in protease allergen-induced airway inflammation. *Immunity.* 36:451–463. https://doi.org/10.1016/j.immuni.2011.12.020

Halim, T.Y., A. MacLaren, M.T. Romanish, M.J. Gold, K.M. McNagny, and F. Takei. 2012b. Retinoic-acid-receptor-related orphan nuclear receptor alpha is required for natural helper cell development and allergic inflammation. *Immunity.* 37:463–474. https://doi.org/10.1016/j.immuni.2012.06.012

Halim, T.Y., C.A. Steer, L. Mathä, M.J. Gold, I. Martinez-Gonzalez, K.M. McNagny, A.N. McKenzie, and F. Takei. 2014. Group 2 innate lymphoid cells are critical for the initiation of adaptive T helper 2 cell-mediated allergic lung inflammation. *Immunity.* 40:425–435. https://doi.org/10.1016/j.immuni.2014.01.011

Hatfield, C.A., J.R. Brashler, G.E. Winterrowd, F.P. Bell, R.L. Griffin, S.F. Fidler, K.P. Kolbasa, J.L. Mobley, K.L. Shull, I.M. Richards, and J.E. Chin. 1997. Intercellular adhesion molecule-1-deficient mice have antibody responses but impaired leukocyte recruitment. *Am. J. Physiol.* 273:L513–L523. https://doi.org/10.1152/ajplung.1997.273.3.L513

Hogg, N., I. Patzak, and F. Willenbrock. 2011. The insider's guide to leukocyte integrin signalling and function. *Nat. Rev. Immunol.* 11:416–426. https://doi.org/10.1038/nri2986

Hoyler, T., C.S. Klose, A. Souabni, A. Turqueti-Neves, D. Pfeifer, E.L. Rawlins, D. Voehringer, M. Busslinger, and A. Diefenbach. 2012. The transcription factor GATA-3 controls cell fate and maintenance of type 2 innate lymphoid cells. *Immunity.* 37:634–648. https://doi.org/10.1016/j.immuni.2012.06.020

Hubbard, A.K., and R. Rothlein. 2000. Intercellular adhesion molecule-1 (ICAM-1) expression and cell signaling cascades. *Free Radic. Biol. Med.* 28:1379–1386. https://doi.org/10.1016/S0891-5849(00)00223-9

Iwamoto, I., and A. Nakao. 1995. Induction of Th2 cell tolerance to a soluble antigen by blockade of the LFA-1-dependent pathway prevents allergic inflammation. *Immunol. Res.* 14:263–270. https://doi.org/10.1007/BF02935624

Kamijo, S., H. Takeda, T. Tokura, M. Suzuki, K. Inui, M. Hara, H. Matsuda, A. Matsuda, K. Oboki, T. Ohno, et al. 2013. IL-33-mediated innate response and adaptive immune cells contribute to maximum responses

of protease allergen-induced allergic airway inflammation. *J. Immunol.* 190:4489–4499. https://doi.org/10.4049/jimmunol.1201212

Karta, M.R., P.S. Rosenthal, A. Beppu, C.Y. Vuong, M. Miller, S. Das, R.C. Kurten, T.A. Doherty, and D.H. Broide. 2018. β_2 integrins rather than β_1 integrins mediate Alternaria-induced group 2 innate lymphoid cell trafficking to the lung. *J. Allergy Clin. Immunol.* 141:329–338.e12. https://doi.org/10.1016/j.jaci.2017.03.010

Klose, C.S., and D. Artis. 2016. Innate lymphoid cells as regulators of immunity, inflammation and tissue homeostasis. *Nat. Immunol.* 17:765–774. https://doi.org/10.1038/ni.3489

Koga, S., K. Hozumi, K.I. Hirano, M. Yazawa, T. Terooatea, A. Minoda, T. Nagasawa, S. Koyasu, and K. Moro. 2018. Peripheral PDGFRα$^+$gp38$^+$ mesenchymal cells support the differentiation of fetal liver-derived ILC2. *J. Exp. Med.* 215:1609–1626. https://doi.org/10.1084/jem.20172310

Lee, M.W., J.I. Odegaard, L. Mukundan, Y. Qiu, A.B. Molofsky, J.C. Nussbaum, K. Yun, R.M. Locksley, and A. Chawla. 2015. Activated type 2 innate lymphoid cells regulate beige fat biogenesis. *Cell.* 160:74–87. https://doi.org/10.1016/j.cell.2014.12.011

Lee, Y.C., K.T. Cheon, and Y.K. Rhee. 1997. Changes of soluble ICAM-1 levels in serum and bronchoalveolar lavage fluid from patients with atopic bronchial asthma after allergen challenge. *J. Asthma.* 34:405–412. https://doi.org/10.3109/02770909709055382

Li, B.W., M.J. de Bruijn, I. Tindemans, M. Lukkes, A. KleinJan, H.C. Hoogsteden, and R.W. Hendriks. 2016. T cells are necessary for ILC2 activation in house dust mite-induced allergic airway inflammation in mice. *Eur. J. Immunol.* 46:1392–1403. https://doi.org/10.1002/eji.201546119

Li, Y.F., Y.H. Tsao, W.J. Gauderman, D.V. Conti, E. Avol, L. Dubeau, and F.D. Gilliland. 2005. Intercellular adhesion molecule-1 and childhood asthma. *Hum. Genet.* 117:476–484. https://doi.org/10.1007/s00439-005-1319-7

Liu, B., J.B. Lee, C.Y. Chen, G.K. Hershey, and Y.H. Wang. 2015. Collaborative interactions between type 2 innate lymphoid cells and antigen-specific CD4+ Th2 cells exacerbate murine allergic airway diseases with prominent eosinophilia. *J. Immunol.* 194:3583–3593. https://doi.org/10.4049/jimmunol.1400951

Maazi, H., N. Patel, I. Sankaranarayanan, Y. Suzuki, D. Rigas, P. Soroosh, G.J. Freeman, A.H. Sharpe, and O. Akbari. 2015. ICOS:ICOS-ligand interaction is required for type 2 innate lymphoid cell function, homeostasis, and induction of airway hyperreactivity. *Immunity.* 42:538–551. https://doi.org/10.1016/j.immuni.2015.02.007

Martinez-Gonzalez, I., C.A. Steer, and F. Takei. 2015. Lung ILC2s link innate and adaptive responses in allergic inflammation. *Trends Immunol.* 36:189–195. https://doi.org/10.1016/j.it.2015.01.005

McKenzie, A.N.J., H. Spits, and G. Eberl. 2014. Innate lymphoid cells in inflammation and immunity. *Immunity.* 41:366–374. https://doi.org/10.1016/j.immuni.2014.09.006

Mielke, L.A., S.A. Jones, M. Raverdeau, R. Higgs, A. Stefanska, J.R. Groom, A. Misiak, L.S. Dungan, C.E. Sutton, G. Streubel, et al. 2013. Retinoic acid expression associates with enhanced IL-22 production by γδ T cells and innate lymphoid cells and attenuation of intestinal inflammation. *J. Exp. Med.* 210:1117–1124. https://doi.org/10.1084/jem.20121588

Mirchandani, A.S., A.G. Besnard, E. Yip, C. Scott, C.C. Bain, V. Cerovic, R.J. Salmond, and F.Y. Liew. 2014. Type 2 innate lymphoid cells drive CD4+ Th2 cell responses. *J. Immunol.* 192:2442–2448. https://doi.org/10.4049/jimmunol.1300974

Mjösberg, J., J. Bernink, K. Golebski, J.J. Karrich, C.P. Peters, B. Blom, A.A. te Velde, W.J. Fokkens, C.M. van Drunen, and H. Spits. 2012. The transcription factor GATA3 is essential for the function of human type 2 innate lymphoid cells. *Immunity.* 37:649–659. https://doi.org/10.1016/j.immuni.2012.08.015

Monticelli, L.A., M.D. Buck, A.L. Flamar, S.A. Saenz, E.D. Tait Wojno, N.A. Yudanin, L.C. Osborne, M.R. Hepworth, S.V. Tran, H.R. Rodewald, et al. 2016. Arginase 1 is an innate lymphoid-cell-intrinsic metabolic checkpoint controlling type 2 inflammation. *Nat. Immunol.* 17:656–665. https://doi.org/10.1038/ni.3421

Moro, K., H. Kabata, M. Tanabe, S. Koga, N. Takeno, M. Mochizuki, K. Fukunaga, K. Asano, T. Betsuyaku, and S. Koyasu. 2016. Interferon and IL-27 antagonize the function of group 2 innate lymphoid cells and type 2 innate immune responses. *Nat. Immunol.* 17:76–86. https://doi.org/10.1038/ni.3309

Mukhopadhyay, S., P. Malik, S.K. Arora, and T.K. Mukherjee. 2014. Intercellular adhesion molecule-1 as a drug target in asthma and rhinitis. *Respirology.* 19:508–513. https://doi.org/10.1111/resp.12285

Nakajima, H., H. Sano, T. Nishimura, S. Yoshida, and I. Iwamoto. 1994. Role of vascular cell adhesion molecule 1/very late activation antigen 4 and intercellular adhesion molecule 1/lymphocyte function-associated antigen 1 interactions in antigen-induced eosinophil and T cell recruitment into the tissue. *J. Exp. Med.* 179:1145–1154. https://doi.org/10.1084/jem.179.4.1145

Nakao, A., H. Nakajima, H. Tomioka, T. Nishimura, and I. Iwamoto. 1994. Induction of T cell tolerance by pretreatment with anti-ICAM-1 and anti-lymphocyte function-associated antigen-1 antibodies prevents antigen-induced eosinophil recruitment into the mouse airways. *J. Immunol.* 153:5819–5825.

Oboki, K., T. Ohno, N. Kajiwara, K. Arae, H. Morita, A. Ishii, A. Nambu, T. Abe, H. Kiyonari, K. Matsumoto, et al. 2010. IL-33 is a crucial amplifier of innate rather than acquired immunity. *Proc. Natl. Acad. Sci. USA.* 107:18581–18586. https://doi.org/10.1073/pnas.1003059107

Qin, A., W. Cai, T. Pan, K. Wu, Q. Yang, N. Wang, Y. Liu, D. Yan, F. Hu, P. Guo, et al. 2013. Expansion of monocytic myeloid-derived suppressor cells dampens T cell function in HIV-1-seropositive individuals. *J. Virol.* 87:1477–1490. https://doi.org/10.1128/JVI.01759-12

Ramos, T.N., D.C. Bullard, and S.R. Barnum. 2014. ICAM-1: isoforms and phenotypes. *J. Immunol.* 192:4469–4474. https://doi.org/10.4049/jimmunol.1400135

Riedel, J.H., M. Becker, K. Kopp, M. Düster, S.R. Brix, C. Meyer-Schwesinger, L.A. Kluth, A.C. Gnirck, M. Attar, S. Krohn, et al. 2017. IL-33-Mediated Expansion of Type 2 Innate Lymphoid Cells Protects from Progressive Glomerulosclerosis. *J. Am. Soc. Nephrol.* 28:2068–2080. https://doi.org/10.1681/ASN.2016080877

Roediger, B., R. Kyle, K.H. Yip, N. Sumaria, T.V. Guy, B.S. Kim, A.J. Mitchell, S.S. Tay, R. Jain, E. Forbes-Blom, et al. 2013. Cutaneous immunosurveillance and regulation of inflammation by group 2 innate lymphoid cells. *Nat. Immunol.* 14:564–573. https://doi.org/10.1038/ni.2584

Salomon, B., and J.A. Bluestone. 1998. LFA-1 interaction with ICAM-1 and ICAM-2 regulates Th2 cytokine production. *J. Immunol.* 161:5138–5142.

Scholer, A., S. Hugues, A. Boissonnas, L. Fetler, and S. Amigorena. 2008. Intercellular adhesion molecule-1-dependent stable interactions between T cells and dendritic cells determine CD8+ T cell memory. *Immunity.* 28:258–270. https://doi.org/10.1016/j.immuni.2007.12.016

Seehus, C., and J. Kaye. 2016. *In vitro* Differentiation of Murine Innate Lymphoid Cells from Common Lymphoid Progenitor Cells. *Bio Protoc.* 6:e1770. https://doi.org/10.21769/BioProtoc.1770

Seehus, C.R., P. Aliahmad, B. de la Torre, I.D. Iliev, L. Spurka, V.A. Funari, and J. Kaye. 2015. The development of innate lymphoid cells requires TOX-dependent generation of a common innate lymphoid cell progenitor. *Nat. Immunol.* 16:599–608. https://doi.org/10.1038/ni.3168

Serafini, N., C.A. Vosshenrich, and J.P. Di Santo. 2015. Transcriptional regulation of innate lymphoid cell fate. *Nat. Rev. Immunol.* 15:415–428. https://doi.org/10.1038/nri3855

Shi, M., G. Shi, J. Tang, D. Kong, Y. Bao, B. Xiao, C. Zuo, T. Wang, Q. Wang, Y. Shen, et al. 2014. Myeloid-derived suppressor cell function is diminished in aspirin-triggered allergic airway hyperresponsiveness in mice. *J. Allergy Clin. Immunol.* 134:1163–74.e16. https://doi.org/10.1016/j.jaci.2014.04.035

Spooner, C.J., J. Lesch, D. Yan, A.A. Khan, A. Abbas, V. Ramirez-Carrozzi, M. Zhou, R. Soriano, J. Eastham-Anderson, L. Diehl, et al. 2013. Specification of type 2 innate lymphocytes by the transcriptional determinant Gfi1. *Nat. Immunol.* 14:1229–1236. https://doi.org/10.1038/ni.2743

Springer, T.A. 1990. The sensation and regulation of interactions with the extracellular environment: the cell biology of lymphocyte adhesion receptors. *Annu. Rev. Cell Biol.* 6:359–402. https://doi.org/10.1146/annurev.cb.06.110190.002043

Stanciu, L.A., and R. Djukanovic. 1998. The role of ICAM-1 on T-cells in the pathogenesis of asthma. *Eur. Respir. J.* 11:949–957. https://doi.org/10.1183/09031936.98.11040949

Suzuki, M., R. Morita, Y. Hirata, T. Shichita, and A. Yoshimura. 2015. Spred1, a Suppressor of the Ras-ERK Pathway, Negatively Regulates Expansion and Function of Group 2 Innate Lymphoid Cells. *J. Immunol.* 195:1273–1281. https://doi.org/10.4049/jimmunol.1500531

Tang, M.L., and L.C. Fiscus. 2001. Important roles for L-selectin and ICAM-1 in the development of allergic airway inflammation in asthma. *Pulm. Pharmacol. Ther.* 14:203–210. https://doi.org/10.1006/pupt.2001.0293

Tang, R.B., S.J. Chen, W.J. Soong, and R.L. Chung. 2002. Circulating adhesion molecules in sera of asthmatic children. *Pediatr. Pulmonol.* 33:249–254. https://doi.org/10.1002/ppul.10063

Taylor, S., Y. Huang, G. Mallett, C. Stathopoulou, T.C. Felizardo, M.A. Sun, E.L. Martin, N. Zhu, E.L. Woodward, M.S. Elias, et al. 2017. PD-1 regulates KLRG1$^+$ group 2 innate lymphoid cells. *J. Exp. Med.* 214:1663–1678. https://doi.org/10.1084/jem.20161653

Walker, J.A., and A.N.J. McKenzie. 2018. T_H2 cell development and function. *Nat. Rev. Immunol.* 18:121–133. https://doi.org/10.1038/nri.2017.118

Walker, J.A., J.L. Barlow, and A.N. McKenzie. 2013. Innate lymphoid cells--how did we miss them? *Nat. Rev. Immunol.* 13:75–87. https://doi.org/10.1038/nri3349

Wang, S., P. Xia, Y. Chen, Y. Qu, Z. Xiong, B. Ye, Y. Du, Y. Tian, Z. Yin, Z. Xu, and Z. Fan. 2017. Regulatory Innate Lymphoid Cells Control Innate Intestinal Inflammation. *Cell.* 171:201–216.e18. https://doi.org/10.1016/j.cell.2017.07.027

Wegner, C.D., R.H. Gundel, P. Reilly, N. Haynes, L.G. Letts, and R. Rothlein. 1990. Intercellular adhesion molecule-1 (ICAM-1) in the pathogenesis of asthma. *Science.* 247:456–459. https://doi.org/10.1126/science.1967851

Wolyniec, W.W., G.T. De Sanctis, G. Nabozny, C. Torcellini, N. Haynes, A. Joetham, E.W. Gelfand, J.M. Drazen, and T.C. Noonan. 1998. Reduction of antigen-induced airway hyperreactivity and eosinophilia in ICAM-1-deficient mice. *Am. J. Respir. Cell Mol. Biol.* 18:777–785. https://doi.org/10.1165/ajrcmb.18.6.3056

Wong, S.H., J.A. Walker, H.E. Jolin, L.F. Drynan, E. Hams, A. Camelo, J.L. Barlow, D.R. Neill, V. Panova, U. Koch, et al. 2012. Transcription factor RORα is critical for nuocyte development. *Nat. Immunol.* 13:229–236. https://doi.org/10.1038/ni.2208

Yagi, R., C. Zhong, D.L. Northrup, F. Yu, N. Bouladoux, S. Spencer, G. Hu, L. Barron, S. Sharma, T. Nakayama, et al. 2014. The transcription factor GATA3 is critical for the development of all IL-7Rα-expressing innate lymphoid cells. *Immunity.* 40:378–388. https://doi.org/10.1016/j.immuni.2014.01.012

Yamashita, M., R. Shinnakasu, H. Asou, M. Kimura, A. Hasegawa, K. Hashimoto, N. Hatano, M. Ogata, and T. Nakayama. 2005. Ras-ERK MAPK cascade regulates GATA3 stability and Th2 differentiation through ubiquitin-proteasome pathway. *J. Biol. Chem.* 280:29409–29419. https://doi.org/10.1074/jbc.M502333200

Yang, Q., L.A. Monticelli, S.A. Saenz, A.W. Chi, G.F. Sonnenberg, J. Tang, M.E. De Obaldia, W. Bailis, J.L. Bryson, K. Toscano, et al. 2013. T cell factor 1 is required for group 2 innate lymphoid cell generation. *Immunity.* 38:694–704. https://doi.org/10.1016/j.immuni.2012.12.003

Yu, X., Y. Wang, M. Deng, Y. Li, K.A. Ruhn, C.C. Zhang, and L.V. Hooper. 2014. The basic leucine zipper transcription factor NFIL3 directs the development of a common innate lymphoid cell precursor. *eLife.* 3. https://doi.org/10.7554/eLife.04406

Zhang, J., J.C. Grindley, T. Yin, S. Jayasinghe, X.C. He, J.T. Ross, J.S. Haug, D. Rupp, K.S. Porter-Westpfahl, L.M. Wiedemann, et al. 2006. PTEN maintains haematopoietic stem cells and acts in lineage choice and leukaemia prevention. *Nature.* 441:518–522. https://doi.org/10.1038/nature04747

Zhong, C., and J. Zhu. 2017. Transcriptional regulators dictate innate lymphoid cell fates. *Protein Cell.* 8:242–254. https://doi.org/10.1007/s13238-017-0369-7

Zook, E.C., and B.L. Kee. 2016. Development of innate lymphoid cells. *Nat. Immunol.* 17:775–782. https://doi.org/10.1038/ni.3481

Zook, E.C., K. Ramirez, X. Guo, G. van der Voort, M. Sigvardsson, E.C. Svensson, Y.X. Fu, and B.L. Kee. 2016. The ETS1 transcription factor is required for the development and cytokine-induced expansion of ILC2. *J. Exp. Med.* 213:687–696. https://doi.org/10.1084/jem.20150851